

AD-A068 366

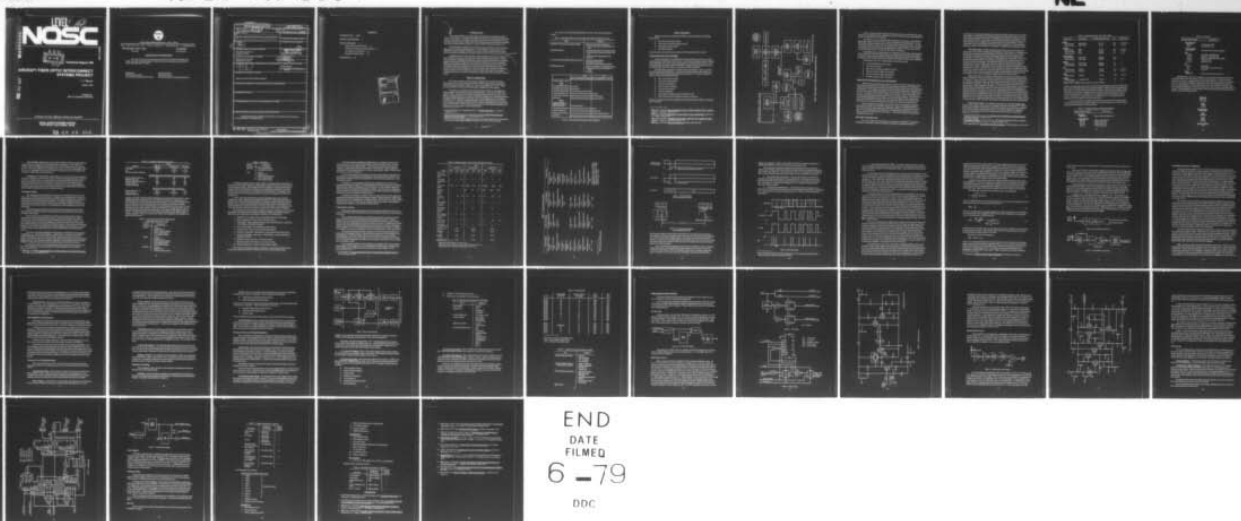
NAVAL OCEAN SYSTEMS CENTER SAN DIEGO CA
AIRCRAFT FIBER-OPTIC INTERCONNECT SYSTEMS PROJECT. (U)
MAR 79 T A MEADOR
NOSC-TR-390

F/G 20/6

UNCLASSIFIED

NL

1 OF 1
AD
AO 398



LEVEL II

42

AD A068366

NOSC

NOSC TR 390



Technical Report 390

AIRCRAFT FIBER-OPTIC INTERCONNECT SYSTEMS PROJECT

T. A. Meador

1 March 1979

Prepared for
Naval Air Systems Command

DDC FILE COPY

APPROVED FOR PUBLIC RELEASE; DISTRIBUTION UNLIMITED

NAVAL OCEAN SYSTEMS CENTER
SAN DIEGO, CALIFORNIA 92152

79 05 09 015



NAVAL OCEAN SYSTEMS CENTER, SAN DIEGO, CA 92162

AN ACTIVITY OF THE NAVAL MATERIAL COMMAND
RR GAVAZZI, CAPT, USN **HL BLOOD**

Commander

Technical Director

ADMINISTRATIVE INFORMATION

The work in this report was sponsored by the Naval Air Systems Command (code 360G) under their Avioptics Program. Work at NOSC was done under project 63257N, W0477-AS, W0477001, 732-SA12.

Released by
CDR WJ Tinston, Head
Air Surveillance Systems Project Office

Under authority of
RE Shuttters, Head
Surface/Aerospace Surveillance Department

UNCLASSIFIED

SECURITY CLASSIFICATION OF THIS PAGE (When Data Entered)

REPORT DOCUMENTATION PAGE		READ INSTRUCTIONS BEFORE COMPLETING FORM	
1. REPORT NUMBER NOSC Technical Report 390 TR-390	2. GOVT ACCESSION NO.	3. RECIPIENT'S CATALOG NUMBER D. Technical kept	
4. TITLE (and Subtitle) AIRCRAFT FIBER-OPTIC INTERCONNECT SYSTEMS PROJECT		5. TYPE OF REPORT & PERIOD COVERED	
7. AUTHOR(s) T. A. Meador		6. PERFORMING ORG. REPORT NUMBER	
9. PERFORMING ORGANIZATION NAME AND ADDRESS Naval Ocean Systems Center San Diego, CA 92152		8. CONTRACT OR GRANT NUMBER(s)	
11. CONTROLLING OFFICE NAME AND ADDRESS Naval Air Systems Command Washington, D.C. 20361		10. PROGRAM ELEMENT, PROJECT, TASK AREA & WORK UNIT NUMBERS 63257N, W0477AS, W0477001 732-SA12	
14. MONITORING AGENCY NAME & ADDRESS (if different from Controlling Office) 1247P.		12. REPORT DATE 1 March 1979	
		13. NUMBER OF PAGES 46	
		15. SECURITY CLASS. (of this report) UNCLASSIFIED	
		15a. DECLASSIFICATION/DOWNGRADING SCHEDULE	
16. DISTRIBUTION STATEMENT (of this Report) Approved for public release; distribution unlimited			
17. DISTRIBUTION STATEMENT (of the abstract entered in Block 20, if different from Report)			
18. SUPPLEMENTARY NOTES			
19. KEY WORDS (Continue on reverse side if necessary and identify by block number)			
20. ABSTRACT (Continue on reverse side if necessary and identify by block number) This report summarizes the development and fabrication of a fiber-optic interconnect intended for use in a MIL-STD-1553 multiplex system.			

DD FORM 1473
1 JAN 73EDITION OF 1 NOV 68 IS OBSOLETE
S/N 0102-LP-014-6601

UNCLASSIFIED

SECURITY CLASSIFICATION OF THIS PAGE (When Data Entered)

393159

CONTENTS

INTRODUCTION . . . page 3

PROJECT DESCRIPTION . . . 3

PHASE I PROGRESS . . . 5

System Documentation Report . . . 5

Fiber-Optic Interconnect Analysis Report . . . 7

Development and Test Plan . . . 27

Breadboard Design Report . . . 33

REFERENCES . . . 44

ACCESSION for	
NTIS	White Section <input checked="" type="checkbox"/>
DOC	Buff Section <input type="checkbox"/>
UNANNOUNCED	<input type="checkbox"/>
JUSTIFICATION _____	
BY _____	
DISTRIBUTION/AVAILABILITY CODES _____	
SPECIAL _____	
A	

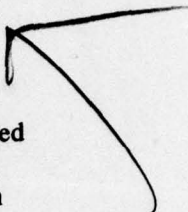


INTRODUCTION

The Avioptics Program is an engineering and application development program whose central objective is to support the preparation of fiber-optic transmission technology for use in naval aircraft. The program has been organized and is being managed by the Air Surveillance Systems Project Office (code 7309) of the Naval Ocean Systems Center (NOSC). The Avioptics Program Plan is presented in detail in NOSC Technical Document 197.¹

The applications of principal interest in the Avioptics Program are the transmission interconnects of aircraft multiplex systems. Included within the scope of this area are digital time division multiplex (TDM) systems, video multiplex and distribution systems, and such equipment ensembles as armaments, flight control, and voice communications.

A significant return on the investment in this program is expected to be realized in the reduction of life-cycle costs associated with aircraft electronic systems.² Factors such as reduction of shielding, filtering, and transceiver design requirements are anticipated together with enhanced resistance to electromagnetic disruption of system transmission. Fiber-optic transmission should raise the quality of system performance in severe mission environments above that achievable in conventionally wired systems under the same conditions. Fiber-optic technology also offers potentially wider transmission bandwidths than are possible with wire technology, a situation which could result in an expanded multiplexing capacity for a system or high-speed or high-quality signal transmission between points.



PROJECT DESCRIPTION

One of the key segments of the Avioptics Program is the Aircraft Fiber-Optic Interconnect Project which is being performed by NOSC personnel and by personnel of IBM Federal Systems Division, Owego, NY, under contract N00123-77-C-0747. NOSC has responsibility for technical and administrative management of this contract.

This project is concerned with the interconnection of both low- and high-speed digital multiplex systems with fiber-optic transmission links. The project consists of two phases of effort: one is devoted to the low-speed digital application and the other to the high-speed digital application. Each phase consists of an analysis and a supporting subphase of hardware design, fabrication, and testing. The low-speed digital system of interest is MIL-STD-1553.* The Phase II high-speed digital system will simulate the projected data transfer requirements and operational features of a future, high performance avionic system such as VSTOL AEW or ASW. A fiber-optic interconnect will be prepared, evaluated, and fabricated to serve the system's transfer requirements.

¹ Naval Ocean Systems Center, Technical Document 197, Avioptics Program Plan, W. J. Tinston, Jr., 25 September 1978.

² Naval Electronics Laboratory Center, Technical Report 1982, A-7 ALOFT Life-Cycle Costs and Measures of Effectiveness Models, R. A. Greenwell, March 1976.

* MIL-STD-1553A defines a digital multiplex avionic system. See draft MIL-STD-1553B, Aircraft Internal Time Division Command/Response Multiplex Data Bus, 16 June 1978, for the latest revision.

An outline of the major project milestones is in table 1 and a project schedule is in figure 1.

Table 1. Principal milestones of the Aircraft Fiber-Optic Interconnect Project.

Phase	Milestone
I: MIL-STD-1553 interconnect analysis and design	Fiber-optic interconnect analysis report Fiber-optic interconnect development and test plan
Ia: Breadboard and test	Interconnect description and breadboard design 3-port breadboard interconnect fabrication and test 16-port interconnect fabrication and test Test report
II. Advanced fiber-optic digital multiplex interconnect	Laboratory system definition Development and test plan Advanced fiber-optic interconnect analysis
Ila: Breadboard and test	Interconnect description and breadboard design Hardware fabrication, test, and analysis of results Test report

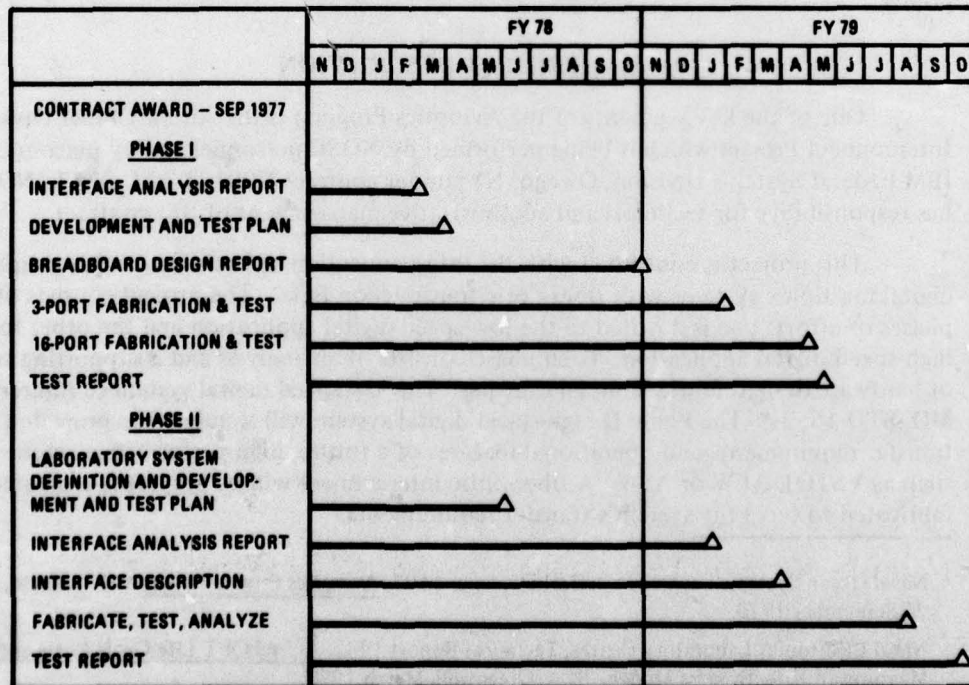


Figure 1. Aircraft fiber-optic interconnect project milestones.

PHASE I PROGRESS

IBM has completed the analysis task of Phase I and has delivered the following task products:

- System documentation report³
- Fiber-optic interconnect analysis report⁴
- Development and test plan⁵
- Breadboard design⁶

These documents are described and summarized in the remainder of this section.

SYSTEM DOCUMENTATION REPORT

This is a description of the IBM laboratory system which is to serve as the experimental test bed for the Phase Ia interconnect. A multiterminal multiplex system, operated under MIL-STD-1553 control, format, and protocol, was required by the contract. It was also required that the system consist of multiplex terminals, a control interface terminal, a twisted/shielded pair interconnect, and an array of avionic equipment.

The IBM system possesses the requisite functional elements — avionics, terminals, and 1553 equipment and operation — as well as an on-line computer facility which can provide system monitoring and functional avionic simulation. The system, illustrated in figure 2, includes the following hardware:

- Two 1553 remote terminals
- One 1553 control terminal
- 1553 data bus hardware
- One bus control computer
- One avionics computer
- Avionics equipment
- One real-time, on-line data entry and retrieval unit
- S370 computer-based simulation laboratory connection

This system equipment is located in IBM's System Integration Facility (SIF) at the Owego, New York, plant.

³ IBM, Report 77-560-001, System Documentation Report of Software Integration Facility: Summary Report, P. A. Wilkinson, 14 October 1977.

⁴ IBM, Report 78-A59-003, Fiber Optic Interconnect Systems: System Analysis Report, R. Betts and R. C. Clapper, 16 March 1978.

⁵ IBM, Report 78-A77-001A, Development and Test Plan for MIL-STD-1553 Compatible Fiber Optic System, V. P. Zeyak, Jr., and R. Betts, 22 March 1978.

⁶ IBM, Report 78-517-002, Breadboard Design Report, R. Betts, 6 November 1978.

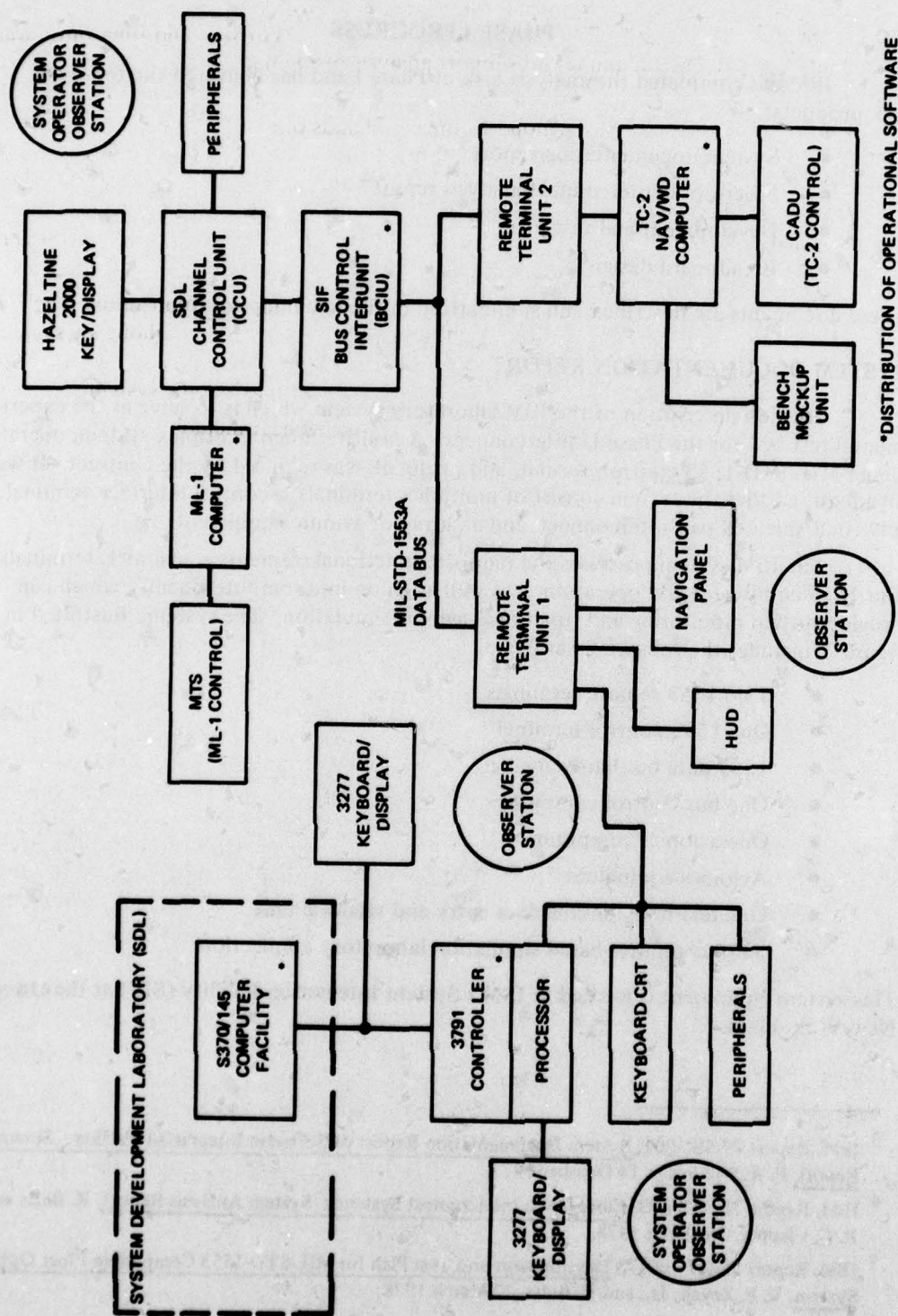


Figure 2. Block diagram of the IBM-FSD System Integration Facility (SIF).

Such an extensive facility will allow side-by-side tests of wire and fiber-optic transmissions to be performed, and it will support analysis of the impact upon system operation caused by substitution of interconnects.

The system is set up to respond to the commands of an observer at the HUD/navigation panel station as if he were an A-7 pilot monitoring aircraft operation in a cockpit. This station interfaces with the data bus through remote terminal unit 1 (RT1). A navigation/weapons delivery computer (TC-2) connects to the bus through RT2. Bus operation is controlled by the ML-1 computer through the BCIU. Other A-7 avionics functions are simulated through the 3791 controller by the S370/145 computer.

The SIF laboratory is representative of a federated tactical avionic system designed around a MIL-STD-1553 wire digital data bus for information transfer among subsystems. An interface with a system development laboratory (SDL) allows the SIF to be configured as desired; simulation data can be made available for the desired avionic system verification.

The elements of the 1553 communication interconnect include

- Twisted/shielded wire pair channel
- Transformer couplers
- Bus control interface unit (BCIU) and ML-1
- Remote terminal 1 (RT1) and interface
- Remote terminal 2 (RT2) and interface
- Software modules in ML-1 and BCIU

FIBER-OPTIC INTERCONNECT ANALYSIS REPORT

This document summarizes the results of a survey of fiber-optic technology, a fiber-optic transmission analysis, and a fiber-optic communications analysis, all of which were undertaken to provide means and methods of specifying fiber-optic interconnect architecture and operation. The principal requirement for the interconnect design was to minimize the effects of interconnect design and operation upon the protocol, format, and control features of 1553. In addition, the interconnect design was to consider, to the extent possible, the environmental requirements which pertain to aircraft electronic systems. The result was to be a proposed design approach for a fiber-optic 1553 interconnect which would include design of the fiber-optic transmission link, encoding and modulation of the optical signal, and analysis of the effects of interconnect operation upon 1553 system performance.

System performance constraints of 1553 have proved to be somewhat unreliable because of the revision of 1553 which is taking place. However, 1553B should have no more effect than does 1553A upon the operation and structure of the fiber-optic interconnect, as the word formats, system architecture, and transmission requirements — all the features affected by the fiber-optic interconnect — of the new standard are fundamentally unchanged from the old.

Fiber-Optic Technology Survey

The survey of fiber-optic components was undertaken to establish the availability, suitability, characteristics, and cost of hardware necessary to assemble the data bus

interconnect. The principal conclusions of the survey were that most activity in the fiber-optic industry is motivated by the telecommunications market and that there is no set of comprehensive guidelines with which to fit together the necessary components for a fiber-optic transmission system. The result is that few militarized system components are available, and those that are available from one manufacturer are not designed to operate in combination with components procured from another manufacturer. Another common problem was found to be the failure of components to fulfill their advertised performance.

Fiber-Optic Cable. The fiber transmission path references the entire fiber-optic interconnect, since all other components are related to its characteristics. All fundamental interconnect requirements and compromises are reflected in the cable's characteristics; the demands of the system being served ultimately determine those requirements and compromises. The fiber-optic interconnect for MIL-STD-1553 must provide a level of conducted optical power sufficient to maintain an acceptable level of detected power for a particular system's bit error rate. The conduction paths are short (less than 100 m) but lossy because of the potentially large number of connectors required for equipments, bulkheads, and couplers. Additionally, the conducted power must be apportioned among a maximum of 32 users. This division of power represents a constant or variable loss which depends upon system architecture. The interconnect must operate in a rather severe environment characterized by extreme temperatures, high mechanical vibration and shock levels, and humidity. All of these considerations rapidly narrow the choice of fibers.

Single-mode fibers are impractical in this application because the transmission path integrity required for efficient conduction is threatened by the mechanical and temperature environment.⁷ Plastic-core fibers are vulnerable to heat and humidity effects. Small source size, which limits available power, and source nonhermeticity deter for the moment the use of single-fiber transmission. Thus, the choice of fiber type is quickly narrowed to multi-mode, glass-core fibers arranged in a bundle form. The bundle array provides a wide physical aperture which can efficiently interface sources whose large emitting areas provide power levels appropriate for the system's bit error rate. Medium-loss fibers (10 to 100 dB/km) do not inflict too large a transmission loss upon the required interconnect, while their numerical apertures (NAs) do not significantly narrow the insertion characteristics of the fiber channel. Additionally, the connector loss of medium-loss fibers is potentially lower than that of high-loss fibers, since their physical dimensions are normally larger and they can be aligned through a keyed connector. Table 2 lists the characteristics of fibers which meet these requirements.

Optical Power Sources. The coupling of optical power from light-emitting diodes (LEDs) or laser diodes to fibers has been extensively analyzed in the literature.^{8,9} Enhancement of source emission characteristics to focus the optical power beam and maximization of the beam intensity are the principal attributes necessary for effectively coupling the amount of power required for system operation into the fiber bundle. The physical

⁷ Standard Telecommunications Laboratory, The Phenomenon of Modal Noise in Analogue and Digital Optical Fiber Systems, R. E. Edworth, 1978.

⁸ Proceedings of the IEEE, vol. 61, no. 12, pp. 1727-1730, "Research Toward Optical-Fiber Transmission Systems, Part II," S. Miller, T. Li, and E. A. J. Marcatili, December 1973.

⁹ RCA, Reprint RE-20-2-13, Optical Fiber Communications Systems, J. D. Wittke, February 1974, pp. 25-27.

Table 2. Component survey: fiber-optic cables.

Manufacturer	Part Number	Core/Clad Dimensions, μm^*	NA	Bundle Count
<u>Galileo</u>				
Glass-clad glass	Gallite 3000	89/110	0.48	1-7-19-37-61
Plastic-clad silica	Gallite "FAT"	204/245	0.35	1-7-19-37
<u>VALTEC</u>				
Glass-clad glass	MS05	65/125	0.26	1-7-19-37
Plastic-clad silica	PC05	125/200	0.3	1-7-19-37
Plastic-clad silica	PC10	250/400	0.3	1-7-19
<u>Quartz Products</u>				
Glass-clad glass	NGS-SI-100	100/150	0.35	1
Plastic-clad silica	QSF-A-200	200/400	0.22	1
<u>DuPont</u>				
Plastic-clad silica	PFX-S-120R	200/600	0.4	1
Plastic-clad silica	PFX-S-220R	200/600	0.4	2
<u>ITT</u>				
Glass-clad glass	GS-02-8	50/125	0.25	1-6-7-19
Plastic-clad silica	PS-05-20	125/300	0.3	1-6-7-19
<u>Times</u>				
Glass-clad glass	SA10-90	90/125	0.16	1-3-6-10
<u>Corning</u>				
Glass-clad glass	Corguide "FAT"	90/125	0.3	1-6-7

*Diameter of fiber core/diameter of fiber measured to outer edge of cladding.

structure and principles of operation of laser diodes and multiheterostructure LEDs provide both devices with high degrees of focussing and intensity. However, these stripe-geometry devices have very small emitting areas which are difficult to locate and to maintain in alignment with fiber channels. In addition, since the humid environment requires the devices to be hermetically sealed the problem of chip alignment within the package becomes critical. This problem is not solved by use of a pigtail fiber, i.e., no hermetically sealed pigtail devices were available at the time of the survey.

The devices which are available and suitable are hermetically sealed, possess large ($> 500 \mu\text{m}$) emitting areas, and utilize some sort of optical enhancement. Typical devices with general characteristics are listed in table 3.

Table 3. Component survey: optical power sources.

Manufacturer/Part Number	Device Type
<u>Spectronics</u>	
SPX-XXXX	Reflector-enhanced edge emitter
<u>Laser Diode Labs</u>	
IRE-140	400- μm surface emitter
IRE-150	240- μm edge emitter
IRE-160	200- μm etched well
IRE-152	100- μm edge emitter

Table 3. Continued.

Manufacturer/Part Number	Device Type
<u>Laser Diode Labs</u>	
IRE-103	Stripe-geometry LED
LCW-5	Stripe-geometry laser
<u>Texas Instruments</u>	
TIXL-XXX	Hemispherical domed emitters/reflector
<u>RCA</u>	
C-30119	Low-power double-HET LED
C-30123	High-power double-HET LED
C-30133	High-power double-HET LED with fiber
C-30127	Low-power laser
C-30130	High-power laser
<u>ITT</u>	
801-E	Stripe LED
851-S	Double-HET surface emitter (hole)
901-L	Stripe laser
<u>Hitachi</u>	
HLP series	400- μ m hemispherical domed emitter

Photodetectors. The devices available for use in optical communications systems are PN photodiodes, PIN photodiodes, and avalanche photodiodes. There are various enhancements, such as coatings and guard rings, which optimize certain device parameters; however, no particular outstanding differences in the optical characteristics of devices exist. For this application, it seems appropriate to use a silicon PIN photodiode because of its simplicity of application, low noise characteristic, low capacitance, and high speed of response. The following list is representative of what is being offered by photodiode manufacturers in silicon PIN photodiodes:

Spectronics

SPX 2232

SPX XXXX

RCA

C-30807

C-30831

Hewlett Packard

5085-4207

EGG

SGD-040-B

UDT

PIN-040

PIN-020

Infrared Industries

7016

Motorola
MRD500

Quantrad
003-PIN-T018

Sharp
PD-50PI

These nine companies offer diodes with active areas either 1 or 0.5 mm in diameter; the diodes are mounted in T018 or T046 hermetic packages. The diameter of the diode's active area is a function of the package and is not optimized for any particular application. If a larger diode is desired, the next size offered is in a T05 package and is approximately 2.5 mm in diameter. Another feature is that the mounting plane in the T046, T018, and T05 package is far from the surface of the package (typically 1.5 to 2.5 mm).

Thus these devices have not been optimized for the proper diameter or mounting plane, but rather they have been optimized only for the packages in which they are mounted. These packages have evolved from the solid-state device market and are not of the optimum configuration for a PIN photodiode. The end result is that output coupling losses are at least 3 dB higher than they should be — strictly because of packaging.

Connectors. Connector manufacturers interested in the telecommunications market produce optical connectors; however, those contacted indicated that they are not willing to pursue the military specification market. The connector manufacturers who normally sell in the military market respond to the commercial fiber-optic market and, although the number of manufacturers is increasing, most are pursuing single-fiber applications at this time. Table 4 lists representative optical connectors.

Table 4. Component survey: optical connectors.

Manufacturer	Device Type
<u>ITT Cannon</u>	
Unilux	Single
SMA-Style	Bundle
<u>Amphenol</u>	
905-119-5006	Bundle (epoxy)
905-119-5014	Bundle (crimp)
906-	Single
<u>Sealectro</u>	
55-907-0149-89	Bundle (SMA)
Prototype	Single in development
<u>Thomas and Betts/Ansley</u>	
998-100	Single
<u>Hughes</u>	
Prototype	Single/Bundle
<u>Deutsch</u>	
Prototype	Single/Bundle

Most manufacturers address the bundle fiber connector with a configuration patterned after an SMA RF coaxial connector. This connector has been shown to be adequate when utilizing high-loss fiber bundles with large numbers of fibers (hundreds). The other device type offered by connector manufacturers is the low-loss single-fiber connector. Various designs have produced connectors in the 1- to 2-dB loss range when adequate control is exercised over fiber diameter. What "adequate control" of fiber diameter actually is can vary from no variation in diameter to a few micrometers. Most single-fiber connectors presently cost from 10 to 100 times that of bundle connectors because they are either prototypes or are in development. The one area not addressed by any manufacturer is a low count fiber bundle connector for medium-loss fibers.

Multiport Couplers. Multiport couplers are truly in the development stage, and only four manufacturers were found who would consider supplying these components.

Table 5 lists these suppliers and describes the coupler types. It should be noted that the coupler survey implicitly limits the system architecture. Two reasons support this limitation: the superior efficiency of star-coupled fiber-optic data bus interconnects has been well established^{10,11} and tee couplers are not as available on short notice as are star couplers.

Table 5. Component survey: multiport couplers.

Manufacturer	Coupler Type
<u>Spectronics</u>	
6 port	Bundle reflective
9 port	Bundle reflective
16 port	Bundle reflective
6 port	Single reflective
9 port	Single reflective
16 port	Single reflective
<u>Galileo</u>	
5 port	Bundle transmissive
9 port	Bundle reflective
16 port	Bundle reflective
<u>ITT</u>	
5 port	Bundle transmissive
9 port	Bundle transmissive
<u>Hughes</u>	
4 port	Single transmissive

In all cases only small numbers of prototype or development hardware have been fabricated. As is shown, most work has been done for bundled fibers and activity is just beginning in single-fiber couplers. Both reflective and transmissive couplers have been fabricated.

¹⁰ AFAL, AFAL-TR-75-45, Optoelectronic Aspects of Avionic Systems, Vol. II, J. R. Biard, May 1975, pp. 70-78.

¹¹ Applied Optics, vol. 15, no. 1, p. 252, "Optical Access Couplers and a Comparison of Multiterminal Fiber Communication Systems," A. F. Milton and A. B. Lee, January 1976.

Rx/Tx Modules. Receiver/transmitter (Rx/Tx) modules have been manufactured by a large number of companies to suit particular system applications. These modules are, without exception, designed for point-to-point links of various length, data rate, and complexity. They are not applicable to a serial data bus system of the type being sought. There is, in fact, no manufacturer of any Rx/Tx module set which claims to have a product that will work in a MIL-STD-1553 serial data bus.

Conclusions. In concluding the component survey, it can be stated that development of optical components is still in a state of flux and that standardization has not yet materialized in any component area. It is expected that as system users define their total system goals and determine realistic specifications for components that a more mature line of component products will evolve. It should be remembered, however, that the largest projected fiber-optic system user will be in the point-to-point telecommunications market and that this market will greatly affect the components industry.

Transmission Analysis

The transmission analysis subjected the results of the component survey to a parametric study of the fiber-optic interconnect. The goal was to develop and use a method for determining the transmission characteristics of an interconnect assembled from an array of components selected for maximum compatibility. The analysis consisted of six steps: a screening process to define the fiber and source types of interest; analysis of the three principal types of interconnect interfaces; a loss budget; and a final screening process to select components.

The screening process classified the multimode fibers according to characteristics and matched the resultant categories with optical power sources selected from the survey of LEDs and laser diodes.

Those sources most compatible with the fiber sets were devices whose emission characteristics have been enhanced with reflectors. The reflectors improve the angular characteristics of emitted power and create circularly symmetric emission patterns. The cost of using reflectors comes in the enlargement of the area occupied by the optical flux. The resultant emitting areas of the sources of interest exceed 1 mm in diameter, which means bundles are most suited in this application where the magnitude of the total power injected into the channel is of overriding importance. Table 6 summarizes the fibers and optical sources.

The choice of the cable configuration was guided by considerations of source/cable compatibility, cost, and physical flexibility. A single fiber is of course the most efficient channel configuration to use with an optical source. However, the sizes of the source emission areas dictate a fiber size in excess of 1 mm which is impractical in terms of flexibility, fragility, and cost. The next most practical configuration is the hexagonally packed bundle of fibers¹² which will match the circular emission patterns of the sources of interest.

Size and fiber count of the hexagonally packed fiber bundles are determined by the size of the emission area of the optical source of interest, the effects of fiber diameter

¹² IBM, Report 75-70-00436, Analysis and Selection of the Physical Parameters of an Optical-Fiber Bundle, R. C. Clapper and R. Betts, October 1975.

Table 6. Grouping of fiber and source types.

Parameter	Fibers		
	High Loss	Medium Loss	Low Loss
Loss, dB/km	100-400	10-40	1-4
NA	38-0.71	0.23-0.45	0.12-0.24
Maximum acceptance angle, deg	47	28	15
Optically Enhanced Sources (Enhanced Surface and Edge Emitters)			
Source emission diameter, μm	400	200	100
Radiation angle, deg	45	27	14
Reflector emission diameter, μm	2000	1400	900
Reflector depth, μm	1200	1400	1500
Coupling to fibers, dB	-7	-4	-
Other Sources (Lasers and Heterojunction Emitters)			
Source emission size, μm	400	200	100
Radiation pattern	Lambertian	Lambertian	$\cos^2\theta$
Coupling to fibers, dB	-16	-11	-5

variation, and limits of fiber flexibility resulting from increasing the fiber diameter. Source emission diameter is a maximum of 1.2 mm for the devices surveyed, which must be at least matched by the cross-sectional area of the fiber bundle. For a set fiber diameter tolerance, the variation in the cross-sectional area of the bundle will diminish when larger numbers of fibers of a given diameter assume the hexagonal pattern of the bundle. A lower fiber diameter size must be imposed to limit connector loss (a few large fibers are easier to maintain in alignment than are many small ones). This minimum fiber diameter was set at 120 μm . The maximum diameter was set at 400 μm (beyond this value fiber flexibility is seriously impaired). Thus the 1.2-mm source emission size dictated the fiber bundle configurations listed in table 7.

Table 7. Typical low count bundle configurations
(source emission area = 1.2 nm).

Variation	Configuration
Minimum	7 fibers Hexagonal N = 3 400- μm maximum diameter 360- μm typical diameter 35- μm possible tolerance
Typical	19 fibers Hexagonal N = 5 240- μm maximum diameter 215- μm typical diameter 20- μm possible tolerance
Maximum	37 fibers Hexagonal N = 7 170- μm maximum diameter

Table 7. Continued.

Variation	Configuration
Maximum	155- μ m typical diameter 15- μ m possible tolerance
Limit	61 fibers Hexagonal N = 9 130- μ m maximum diameter 120- μ m typical diameter 10- μ m possible tolerance

Computer programs were next used to perform transmission efficiency analyses of the source to fiber channel interface, a representative connector interface, and the detector to fiber channel interface. These programs have the capability of stepping through tables of input values for the parameters of interest, and varying these parameters in a random fashion to show the sensitivity of each interface to each parameter. The program results list expected interface loss ranges and order the parameters according to their effects on interface loss.

For the input and output interfaces, device packaging features such as source emission size, source radiation pattern, photodiode diameter, and package depth have the greatest effect. However, the fiber parameters of diameter tolerance, diameter, numerical aperture, and core/clad ratio all affect the input and output interfaces and largely determine the efficiency of connector interfaces. Of lesser importance at each interface are the connector dimensions and tolerances and the parameters associated with end finishing.

The input field for the loss budget calculation program is composed of the parameters listed below. The parameters are entered in minimum, average, and maximum values so that the effects of parameter and performance variations can be determined.

1. LED power: the range of values representing effects of heat and aging
2. Input coupling loss: results of input interface analysis
3. Cable length: length variations resulting from loss characteristics of the fibers and variations in aircraft wiring paths
4. Loss per unit length: fiber transmission characteristics
5. Connector loss: results of connector interface analysis
6. Number of connectors: representative of expected aircraft wiring layouts
7. Number of multiport coupler ports: representative of system specification requirements to date
8. Multiport coupler excess loss: from survey results
9. Multiport coupler nonuniformity: from survey results
10. Output coupling loss: results of output interface analysis

The results of the budget program are maximum, average, and minimum power at the detector in dBm and the power variation at the detector (optical signal range).

In the first complete progression through the series of programs, the parameters used were derived from the general characteristics of devices within the high-, medium-, and low-transmission-loss classes in table 6. The variations and tolerances represented variations in characteristics from device to device. In this manner, a largely qualitative comparison of transmission performance could be made among the classes. Table 8 shows the results of one such comparison.

Once the first results were obtained from the loss budget program, aggregations of specific devices were subjected to the transmission analysis to gauge the sensitivity of the loss budget to changes in specific device parameters. In this way an optimum set of components was derived.

The results of the transmission analysis which established the final selection of system components are in table 9. This final program series is based upon the use of plastic-clad fibers from which the cladding can be removed and a very thin cladding reapplied to reduce connector loss caused by fiber diameter variations. Also necessary is a registration connector which will maintain the hexagonal array of the fibers and preserve the alignment between the arrays in the separate connector halves.

One important implication of table 9 is that the range of detector power places this transmission interconnect within the performance region of PIN photodiodes. High-quality PIN receivers have been designed with -52-dBm sensitivity. Pin detectors are simple, reliable, and much more attractive for use than are avalanche photodiodes which require high bias voltages and are sensitive to heat and bias voltage variations.

Communication Analysis

Project ground rules required the contractor to design an optical fiber interconnect for the 1553 system which would maintain the essential features of system control, protocol, and format.

This is a difficult requirement, as essential aspects of control, protocol, and word format are stated in 1553 in terms of bipolar electrical Manchester code.¹³ Figure 3 illustrates the two word formats defined by the standard; the bipolar waveforms differentiate the word and message types in the first three bits of each word. Intermessage, terminal response, and maximum terminal no-response times are measured by means of the bipolar waveform (figure 4). The word formats and time measurements are necessary to establish 1553 message structure and concomitant features of synchronization, control, and protocol.

True bipolar encoding is difficult to implement in optical fiber transmission since optical power is essentially unipolar. This means that message and word recognition, time synchronization, and gap time measurement in a fiber-optic receiver must be reliably accomplished by means of an optical code which is not the precise analog of the electrical code. Two general approaches are possible; one is inefficient and the other does not follow the rules outlined in 1553.

If the accessible interfaces in 1553 equipments are designed only to accommodate bipolar signals, if the message, word, or synchronization functions require bipolar signals, or if the gap-time measurement can only be performed on bipolar signals, then the

¹³ Draft MIL-STD-1553B, Aircraft Internal Time Division Command/Response Multiplex Data Bus, 16 June 1978, Sections 4.3-4.4.

Table 8. Budget program results for fiber transmission classes.

Input	Fiber								
	Low Loss*			Medium Loss**			High Loss†		
	Min.	Avg.	Max.	Min.	Avg.	Max.	Min.	Avg.	Max.
Enter LED output power, dBm	0	6	10	-5	0	5	-6	0	4
Enter input coupling loss, dB	8	9	10	5	6	7	2	3	4
Enter cable length	0.01	0.1	1.0	0.001	0.01	0.1	0.0001	0.001	0.01
Enter loss, dB/unit length	1	2	4	10	20	40	100	200	400
Enter connector loss, dB	1	1.4	1.8	1.8	2.2	2.2	2.6	3.0	3.4
Enter number of connectors in system	5	6	9	2	4	6	2	3	5
Enter number of ports in system		16			16			16	
Enter multipoint coupler excess loss, dB	3	4	5	2	3	4	1	2	3
Enter nonuniformity, dB	0	2	4	0	1	2	0	0.5	1.0
Enter output coupling loss, dB	1	2	3	2	3	4	3	4	5
Typical power		-31.64			-34.04			-30.74	
Minimum power		-54.24			-53.64			-52.04	
Maximum power		-19.05			-19.65			-19.25	
Dynamic range		35.19			33.99			32.79	

*Single-fiber channel; lengths are 1 km, 100 m, 10 m.

**Bundled fibers, fiber core diameter ~240 μ m, 19 fibers; lengths are 100, 10, 1 m.

†Bundled fibers, fiber core diameter <50 μ m; lengths are 10, 1, 0.1 m.

Table 9. Final system loss analysis.

Input Coupling		Connector Coupling		Output Coupling		System Losses	
Fiber diameter tolerance, $\pm 2.5\%$		Fiber diameter tolerance, $\pm 2.5\%$		Fiber diameter tolerance, $\pm 2.5\%$		LED output power, ± 5 dBm	
Core index of reference, 1.452		Core index of reference, 1.452		Core index of reference, 1.452		Input coupling loss, 5.1 dB	
Fiber diameter/core:clad ratio, 215 $\mu\text{m}/1:1$		Core/clad ratio 1:1		Fiber diameter/core:clad ratio, 215 $\mu\text{m}/1:1$		Cable length, km 0.001 0.01 0.1	
Source diameter, 1.2 mm				Chip diameter (PD), 1 mm		Cable loss, dB/km 10 20 40	
Radiation pattern, $\cos 20^\circ \theta$						Connector loss, 1.3 dB	
Number of fibers, 19		Number of fibers, 19		Number of fibers, 19		Number of connectors, 2 4 6	
Numerical aperture, 0.3		Numerical aperture, 0.3		Numerical aperture, 0.3		Number of ports, 16	
Off-axis tolerance, $\pm 2.5\%$		Off-axis tolerance/rotation, $\pm 2.5\%$		Off-axis tolerance, $\pm 2.5\%$		Coupler excess loss, dB 2 3 4	
Source/fiber separation, 5%*		Bundle/bundle separation, 2.5%*		Bundle/chip separation, 150%*		Coupler nonuniformity, dB 0 1 2	
Angular displacement, 2.5 deg		Angular displacement, 1.0 deg		Angular displacement, 2.5 deg		Output coupling loss, 3.2 dB	
Loss 5.1 dB		Loss 1.3 dB		Loss 3.2 dB		Typical detector power, 29.6 dBm Minimum detector power, 43.1 dBm Maximum detector power, 19.9 dBm Dynamic range, 23.2 dB	

*Percent of fiber bundle diameter

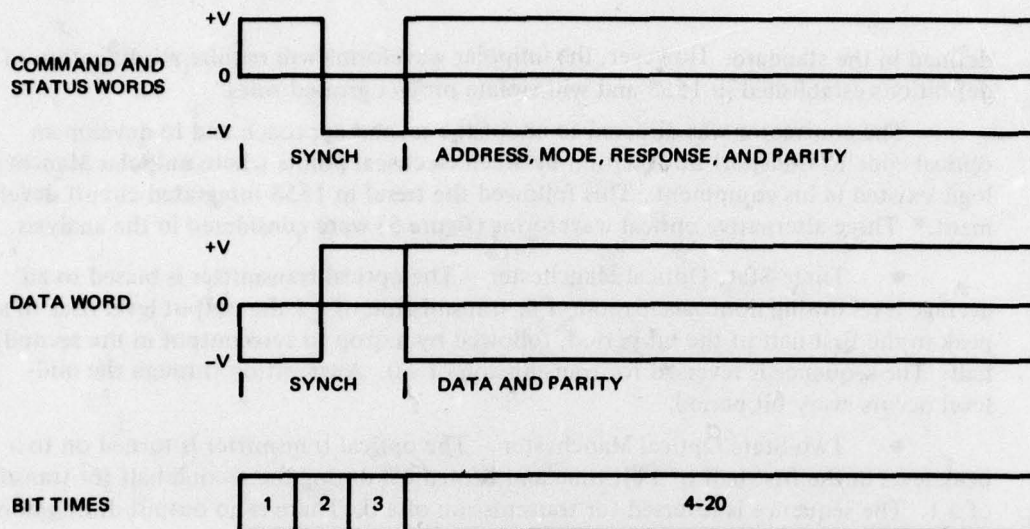


Figure 3. 1553 word formats.
(After Draft MIL-STD-1553B.)

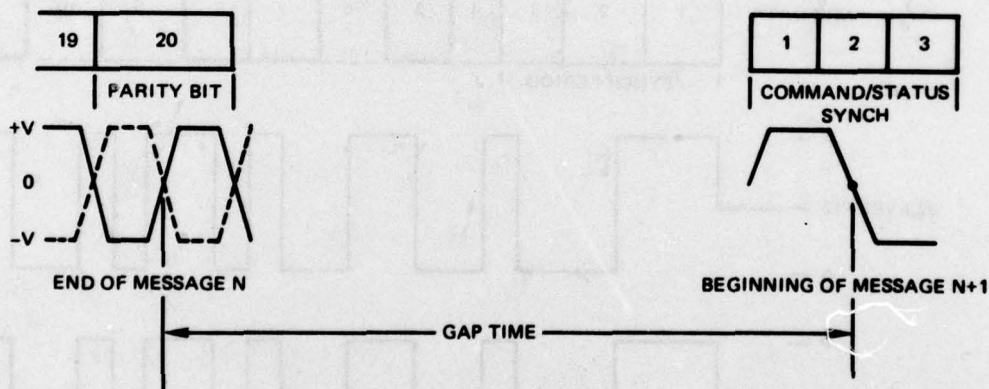


Figure 4. 1553 gap-time measurements.
(After Draft MIL-STD-1553B.)

electrooptical hardware designs will be predetermined in their electrical characteristics. Since bipolar waveforms are available solely at the terminal-to-bus aperture, retaining them in a fiber-optic interconnect design compels the retention of the electrical transceivers necessary to operate the twisted/shielded pair transmission path. Hence, the cost of a fiber-optic interconnect must include the expense of the wire interconnect electrical hardware — hardly a cost effective design.

If the word formats and gap-time measurements are redefined in terms of unipolar electrical logic and if an electrical interface can be located where a unipolar waveform carrying the characteristics of the new definitions exists, then a fiber-optic design can be freed to compete on a one-to-one basis with the bipolar 1553 electrical interconnect

defined in the standard. However, the unipolar waveforms will require modification of definitions established in 1553 and will violate project ground rules.

The contractor was directed to adopt the second approach and to develop an optical code to transport information between electrical points where unipolar Manchester logic existed in his equipment. This followed the trend in 1553 integrated circuit development.* Three alternative optical waveforms (figure 5) were considered in the analysis:

- **Three-State Optical Manchester** – The optical transmitter is biased to an average level during nontransmission. For transmission of a 1 the output level rises to a peak in the first half of the bit period, followed by a drop to zero output in the second half. The sequence is reversed for transmission of a 0. A transition through the mid-level occurs every bit period.
- **Two-State Optical Manchester** – The optical transmitter is turned on to a peak level in the first half of a bit time and turned off during the second half for transmission of a 1. The sequence is reversed for transmission of a 0. There is no output during non-transmission.

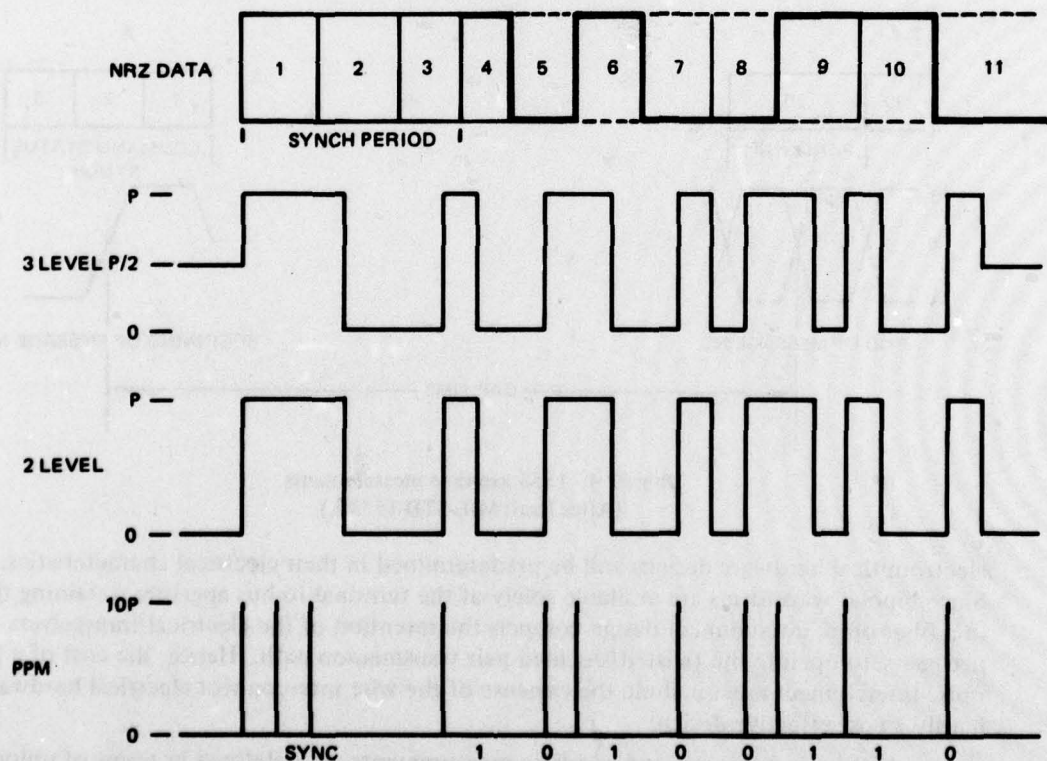


Figure 5. Optical waveforms.

*See the data sheet for the Harris HD-15530 which performs 1553 encoding and decoding functions. Inputs are provided for single- or dual-ended waveforms.

- **Pulse Position Modulation (PPM)** – The optical transmitter emits a string of narrow, high peak level pulses when its activation gate is open during the high level excursions of a positive, unipolar, electrical Manchester signal. The transmitter is off during low Manchester levels.

The three-level code is most analogous to the coding required by MIL-STD-1553 for electrical transmission. It allows a simple optical receiver design where interstage AC coupling can shift the detected signal to a three-state electrical format which pivots about the zero voltage level. This enhances the adaptability of existing electrical receiver technology to the fiber-optic case. Use of this code will permit large optical signal ranges (dynamic ranges) to be accommodated by system receivers, i.e., the average system power level generated by the midlevel outputs of all system transmitters keeps the interstage coupling of all system receivers charged to a constant level and reduces the time required for level shifting between strong and weak signals. This allows the system to enjoy short intermessage gap times which enhances the system transmission efficiency.

The disadvantages of three-state optical Manchester are substantial. The system's constant average power level causes detector shot noise to increase significantly (received signal-to-noise ratio can be reduced by as much as 1.0 to 2.0 dB, depending upon the magnitude of the average power level). Lifetime considerations limit the peak power levels of the optical signal to the levels employed in the two-state code. Thus for a receiver operating with threshold detection the false alarm probability rises above that achievable in the two-level code because the receiver noise figure is higher and the signalling distance is smaller. If laser diodes are used in three-state interconnects, the system's average power level and receiver noise will increase; if APDs are used, the shot noise generated by the background level will be amplified and reduce any gain in receiver sensitivity. Most important, the constant output of system sources will lead to an increase in the rate of source degradation per unit of system operation time, an increase of the average level of electrical power consumption, and increased complexity of transmitter design to achieve intertransmitter output linearity.

Two-state optical Manchester coding, when compared with three-state coding, will provide an increase in receiver signal-to-noise ratio for the same peak optical signal levels. Transmitter design and efficiency are enhanced, and laser diodes and APDs will clearly increase the quality of system operation. The drawbacks of two-state Manchester coding are well known. AC-coupled receivers require a finite amount of time to adjust their stored energy when the average level of detected power changes, as they do when transmission loss is not equalized in every interconnect transmission path. This requires an increase in the minimum intermessage gap time of the system and reduces system transmission efficiency. Two-state coding also requires modification of the 1553 word formats, surrenders the message's error margin during the invalid Manchester word preambles, and increases the complexity of the design of the receiver/detector.

A third alternative exists in the pulse position modulation (PPM) code which can possibly increase receiver signal-to-noise performance by peaking the transmitter output to a value at least 10 times higher than that safely achievable with optical level Manchester codes. Source degradation should be unchanged despite the higher power levels because the short width of the optical pulse (50 ns) and the low average duty cycle (5%) maintain the same average temperature gradient across the source semiconductor junction as is

maintained with the other optical codes.¹⁴ The gain in signal-to-noise ratio for an optical PPM code, assuming the average optical energy per bit remains the same for the pulse as for the level Manchester codes, will be dependent upon the square root of the signal amplitude, since the receiver noise bandwidth is opened at the same rate that the pulse width decreases. The PPM is highly adaptable to use with laser diodes and APDs. The drawbacks of optical PPM are potential RF noise generation by an unshielded transmitter, undetermined sensitivity to high-frequency noise spikes in the system, widened receiver bandwidth, and two levels of coding (unipolar electrical and optical PPM).

A signal-to-noise analysis of the three coding approaches is based upon the following assumptions: (1) the same average power dissipation will be maintained at the LED for each coding approach; (2) a transimpedance amplifier will function as the input stage of the receiver for each coding approach (this establishes the principal noise sources as the preamplifier input stage and the feedback resistor); and (3) the receiver noise is Gaussian.

The RMS noise level present at the filtered output of an amplifier is

$$\sigma = \sqrt{\Phi \int_0^{\infty} [h(u)]^2 du}, \quad (1)$$

where σ is RMS noise level, Φ is noise spectral density, and h is the receiver impulse response. The signal-to-noise ratio at the output of the receiver is

$$\text{SNR} = \frac{A}{\sigma}, \quad (2)$$

where A is the amplitude of an amplified signal, e.g., a pulse. If equation (1) is substituted for σ and equation (2) is multiplied by $S\sqrt{t_1}$ (where S is the amplitude of an input signal and t_1 is the pulsewidth), the SNR becomes

$$\text{SNR} = \frac{\sqrt{S} \cdot \sqrt{St_1}}{\sqrt{\Phi}} \cdot \frac{A}{S\sqrt{t_1} \int_0^{\infty} [h(t)]^2 dt}. \quad (3)$$

In this form, the three pulse codes can be compared on the basis of SNR under the constraint of constant system energy. This constraint will be effective in maintaining a constant temperature gradient across the junction of an LED.

Equation (3) can now be restated as

$$\text{SNR} = \sqrt{S} \cdot C \cdot A_n,$$

where C is a constant determined by the noise characteristics of the receiver and the signal energy present within the system per signalling event; A_n is the normalized received output which is determined by filter characteristics and is always less than unity; and \sqrt{S} is the square root of the input signal level. C is constant for any preamplifier design and is unchanged by coding format, if the system's energy is constant. A_n will vary according to

¹⁴ Spectronics, Inc., Thermal Transients in Light Emitting Diodes, J. R. Biard, 1978. Figure 10.

the filter requirements of the coding approach, but is approximately equal (~ 0.85) for any of the codes.

Now, since \sqrt{S} can be varied without changing the system's energy level, increasing the level of the pulse's input to the amplifier should increase the SNR. Since the PPM mode of operation will allow a much greater pulse amplitude than either of the optical Manchester codes, the SNR of the receiver for PPM operation should be greater than that for the Manchester codes. If the comparison of system performance is made strictly on the basis of SNR resulting from signal amplitude, the apparent superiority of the PPM makes it worthy of evaluation on the basis of an operational comparison with the other optical codes.

Receiver design is also affected in the selection of optical code by the effects of the optical signal range (OSR). The two optical Manchester codes require the receiver gain control to traverse the differences in average power level between messages arriving from different terminals. The PPM receiver can be set to the minimum system signal level; the higher level pulses can be clipped or compressed with simple, fast, reliable circuitry.

Implementation of the PPM is illustrated in figures 6 and 7. The encoder can be adapted to PPM or to two-state Manchester. In the PPM mode of operation it is designed to emit 10-mW-peak, 50-ns-wide pulses spaced 500 ns apart. The pulses are gated by the positive, unipolar 1553 Manchester through a digital counting device. The unipolar Manchester is recaptured at the receiver by feeding the reconstituted pulses into a retriggerable one-shot multivibrator. This receiver multivibrator can be implemented with digital counting logic. The receiver characteristics also include a 7-MHz-wide filter ($f_L = 1$ MHz, $f_H = 8$ MHz) designed to pass that part of the spectrum where most of the pulse power is concentrated. The filter characteristics include two zeroes at 8 MHz.

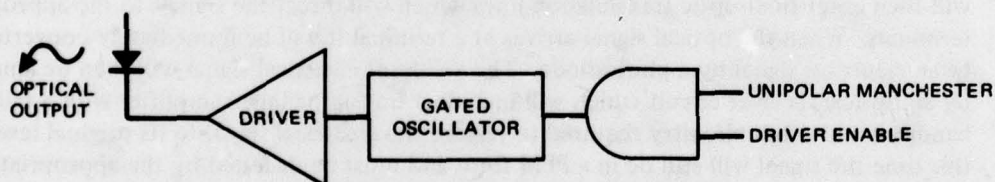


Figure 6. Optical PPM encoder/decoder.

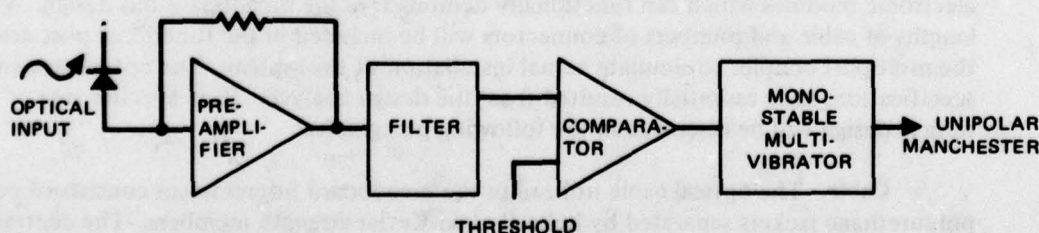


Figure 7. Optical PPM receiver/decoder.

Fiber-Optic Interconnect Configuration

The hardware block diagram for the 1553 fiber-optic interconnect which will be evaluated in IBM's SIF laboratory is shown in figure 8. The subsystem inputs can be either single-ended unipolar signals or dual-ended inputs designed to feed the electrical 1553 transmitters. Output signals with the same characteristics can be provided for the fiber-optic receiver/decoder for use by the subsystem equipments. The terminals consist of encoding and decoding circuits along with the required optical driver and optical receiver circuits. These terminal circuits interface with the optical conversion devices – the light-emitting diode and the photodiode – which in turn interface with the optical bus itself. The optical bus consists of the 16-port transmissive optical coupler, the interconnecting fiber-optic transmission lines, and connectors. The system will be functionally configured as shown to demonstrate various numbers of connectors and transmission line lengths. As designated in the analysis, paths with from two to six in-line connectors will be demonstrated. The length of the transmission line will also be varied to demonstrate operational lengths of as little as 1 m, typical usage of 10 m, and as much as 100 m. By functionally demonstrating the system in these configurations, practical implementation within the scope of MIL-STD-1553 will be shown.

The remote terminal encode/decode circuits will produce PPM, 50-ns, pulse waveforms from the input data waveforms. These PPM waveforms will then modulate the LED via the driver circuits which will be high-frequency peaked to produce a minimum risetime pulse of 1 A with a duration of 50 ns. The optical power from the LED will be coupled to a 19-fiber-bundle, fiber-optic transmission line. The transmission line will direct this optical power to the 16-port transmissive optical coupler which will divide the power equally between the 16 ports. The divided power leaving the output ports of the coupler will then enter fiber-optic transmission lines which will direct the signals to the appropriate terminals. When the optical signal arrives at a terminal it will be immediately converted to an electrical signal by a photodiode. The resultant electrical signal will then be amplified by an optical receiver circuit which will include a transimpedance amplifier with a tailored bandpass and other circuitry required to restore the electrical signal to its original level. At this time the signal will still be in a PPM form and must be decoded by the appropriate circuitry to produce the original, typical 1553 analog signal.

The breadboard fiber-optic transmission link will be a 16-port system interconnected by a transmissive multiport coupler. Three ports of the system will be activated by terminal electronic modules which can functionally demonstrate the breadboard bus design. Various lengths of cable and numbers of connectors will be included in the functional port arms of the multiport coupler to simulate actual installation of the system. The optical design specifications have essentially resulted from the design analysis. Each specific area of the optical design will be discussed in the following paragraphs.

Cable. The optical cable utilized in the breadboard interconnect consists of coaxial polyurethane jackets separated by helically laid Kevlar strength members. The central cavity is filled with 19 plastic-clad fused-silica fibers. Each fiber consists of a $215\text{-}\mu\text{m} \pm 12\text{-}\mu\text{m}$ core of Supersil II fused quartz 3 with a Sylguard 184 plastic cladding. Fiber loss is specified at 10 to 70 dB/km over the optical bandwidth of interest (800 to 900 nm). The core/clad combination gives a numerical aperture of 0.3 and allows the cladding to be easily removed

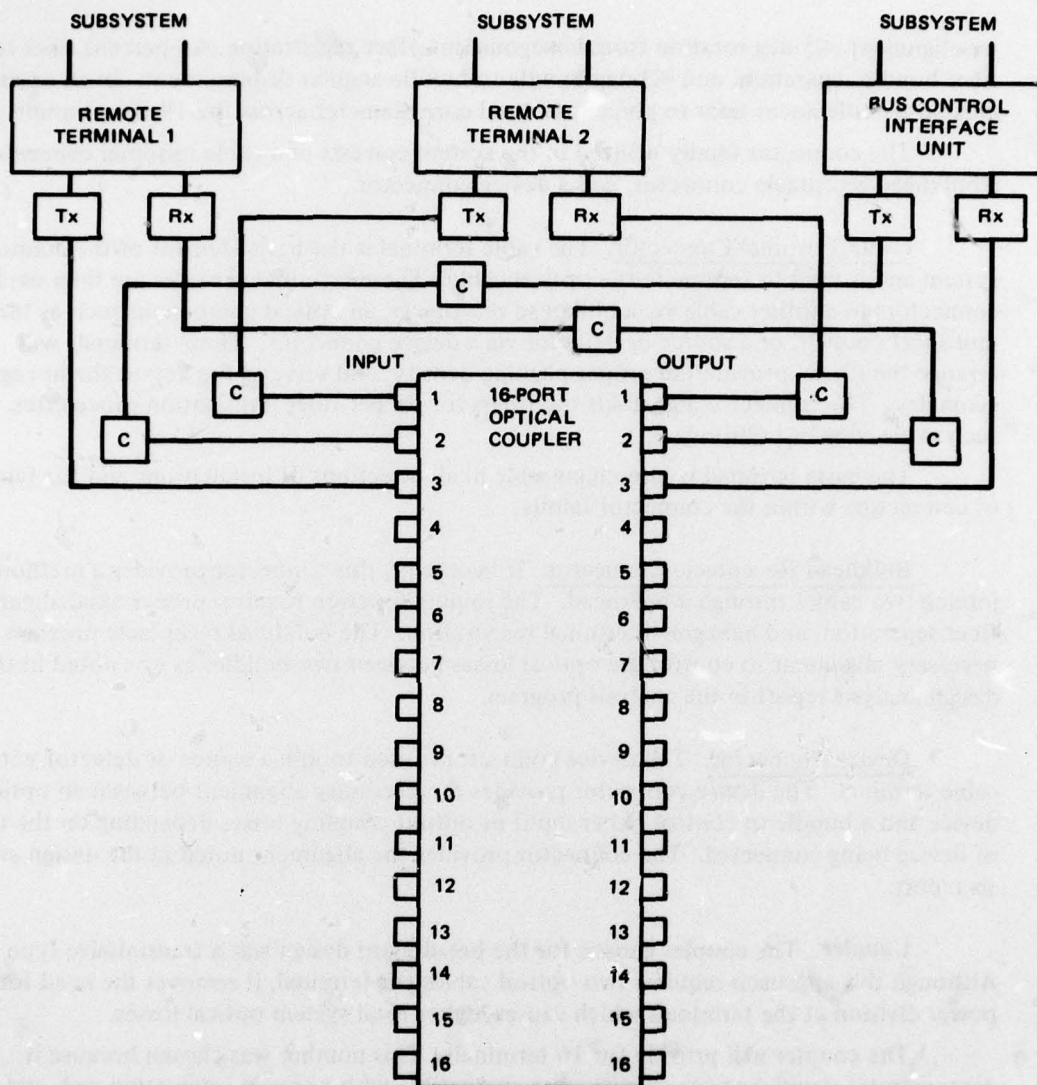


Figure 8. Optical interconnect system hardware.

for termination. The type of cable chosen was a modified version of ITT Electro-Optical Products Division's type ESM-10-PS.

Connectors. The connector chosen was a modified version of ITT Cannon's type MIL-C-85044. The connector has the general profile of an SMA-type RF connector. The terminal portion has been modified so that it has a hexagonal geometrical opening that will properly arrange 19 fibers with core diameters of $215 \mu\text{m} \pm 10 \mu\text{m}$ in a true hexagonal pattern. The connector terminal is also modified within a compatible bulkhead connector to within 5 deg. These two modifications enable the connector terminals to have a high packing fraction (hexagonal geometry) and a low registration loss (connector key). The connector dimensions provide for ≤ 5 -percent fiber diameter tolerance, ≤ 5 -percent axial

misalignment, ≤ 5 -deg rotation from hexagonal interface registration, ≤ 5 -percent fiber-to-fiber bundle separation, and ≤ 3 -deg bundle-to-bundle angular displacement. In all cases percentage tolerances refer to percent of total core diameter across the 19-fiber bundle.

The connector family utilized in the system consists of a cable terminal connector, a bulkhead receptacle connector, and a device connector.

Cable Terminal Connector. The cable terminal is the basic element of the connector system and is used to terminate the optical cable. These terminated cables are then used as connectors to another cable via a bulkhead receptacle, an optical component such as the multiport coupler, or a source or detector via a device connector. These terminals will arrange the fibers, provide the proper packing density, and serve as the key to the hexagonal geometry. The connector also holds the fibers for proper fiber termination procedures, such as cleaving or polishing.

The basic terminal is interchangeable in all directions of installations and for types of connectors within the connector family.

Bulkhead Receptacle Connector. If necessary, this connector provides a method for joining two cables through a bulkhead. The joining function requires proper axial alignment, fiber separation, and hexagonal terminal registration. The bulkhead receptacle provides the necessary alignment to control the optical losses between two bundles as was noted in the design analysis report in the analysis program.

Device Connector. The device connector is used to join a source or detector with a cable terminal. The device connector provides the necessary alignment between an optical device and a bundle to control either input or output coupling losses depending on the type of device being connected. The connector provides the alignment noted in the design analysis report.

Coupler. The coupler chosen for the breadboard design was a transmissive type. Although this approach requires two optical cables per terminal, it removes the need for power division at the terminals which causes higher total system optical losses.

The coupler will provide for 16 terminals. This number was chosen because it demonstrates significant complexity, was compatible with a square integration rod, and would have a loss of only 3 dB from a 32-port device. Cost was also a consideration, since the coupler's cost would not only increase but activation of a 32-port system would be excessive for this demonstration program.

The coupler chosen was a Spectronics type SPX3028. A minor modification will be necessary to allow the use of ITT Cannon's MIL-C-85044 type connector. The specifications of this device are within the requirements set forth in the design analysis.

Optical Source. The optical source chosen for the breadboard design was the Spectronics type SE2231. The dash number 003 device which specifies a minimum of 1.25 mW of power was selected; however, the dash number 002 device (0.95 mW) will also most likely be adequate. The device should not be degraded by 1-A pulses of short duration and duty cycle. The device exhibits a beam angle radiation pattern within the acceptance core angle defined by the fiber NA which is 0.3. The device responds to a 50-ns current pulse.

The physical aperture of the device is compatible with a 1.14-mm fiber bundle diameter. The device emits in the IR region and is compatible with both the fiber and photodiode types chosen. The package can be a TO-18 or TO-46 profile and must provide controlled chip placement features. The device package must be hermetic.

Optical Detector. The detector is a PIN photodiode with a typical responsivity of 0.5 A/W at 907 nm. It has suitable speed ($t_r = 5.5$ ns) at 15-V reverse bias. The physical aperture of the detector is compatible with the bundle diameter of 1.14 mm, and a condensing core is utilized to provide a 70° field-of-view and to desensitize the bundle-to-detector coupling loss. The detector is hermetically sealed and is electrically isolated from its case which can be grounded. The Spectronics silicone PIN photodiode type SD3478 was selected for this application.

DEVELOPMENT AND TEST PLAN

This document describes the test plan by which the 1553 compatible fiber-optic interconnect will be demonstrated and tested. The interconnect is to be tested at the SIF facility. Testing will consist of three levels: component, subsystem, and laboratory system.

Component level testing will be undertaken before assembly of the interconnect hardware to verify that the received components are within their design specifications. The purpose of specifying and conducting these tests is to develop simple methods which produce repeatable, accurate results which can be utilized by a system or circuit engineer when designing or assembling equipment. The components to be tested include: source, detector, cable, connectors, and multipoint coupler.

Subsystem level testing is intended to verify the transfer characteristics of transmission and reception hardware and the transmission function of the PPM link.

Laboratory level tests are intended to validate the functional compatibility of the 1553 multiplex system and the fiber-optic interconnect. Before installation of the interconnect, the laboratory twisted/shielded pair 1553 interconnect will be operated in the A-7 system to establish a functional baseline. The fiber-optic interconnect will then be installed and operated with the same system program. Any differences in system performance will be noted and analyzed to determine whether the effect can be linked to the interconnect change.

Component Level Testing Requirements

Each component will be tested to verify that it meets the listed requirements. Testing will be done at the operation point of the fiber-optic interconnect for each component.

Light-Emitting Diodes. Each LED will be tested for total output at 100-mA continuous forward current. Measurement will be made with an integrating cube. After measurement of input coupling and output coupling and characterization of the receiver amplifier, peak level outputs and rise and fall times will be measured for each LED.

Input Coupling. A short section of mode-stripped cable which has been terminated at each end with connectors will be used to measure input coupling loss, i.e., the loss

encountered between LED and transmission cable. One end of the cable will be joined to an LED through the device connector and the other end will be placed at the aperture of the integrating cube. The loss will be the ratio between the LED measurement described above and the measurement obtained from this procedure.

Output Coupling. The same short section of cable will be used to measure the output coupling loss: the loss experienced between the transmission cable and the photodiode. For this test, the transimpedance preamplifier to be used in the system receiver and the selected system photodiode will also be utilized. Before the test is initiated, the preamplifier's characteristics of transimpedance and noise will be accurately determined and the photodiode's dark current at the bias of interest will be measured. Photodiode responsivity will be accepted from the device data sheet, since the optical measurements required for accurate determination are beyond the scope of this test. The free end of the mode-stripped cable will be joined to the photodiode through the device connector. Output coupling loss will be the ratio of optical power sensed at the photodiode – determined by the quotient of the preamplifier's output voltage and the product of photodiode responsivity and the preamplifier's transimpedance – and the power measured in the integrating cube in the previous test.

Cable Measurement. The calibrated transmitter/receiver combination, achieved by the tests discussed for LEDs, input coupling, and output coupling, can be used to measure the apparent transmission loss of fiber-optic cables of various lengths. This is done by taking the ratio of the transmitted power through the length of the mode-stripped cable of interest to the level of power measured through the short length of cable used in the test for output coupling. Measurements on lengths of at least 1, 10, and 100 m will be made.

Connector Measurement. The calibrated cables obtained in the previous test will be connected through bulkhead connectors and between the calibrated transmitter/receiver pair. The ratio of the apparent transmissivity through the connected sections to the product of their transmissivities, measured in the previous test, will give the loss of the connector.

Multiport Connector. The intrinsic loss of the multiport coupler can be measured by substituting the coupler for the middle of three connected sections of cable used in the previous test. All possible combinations of input and output ports should be measured to determine both the intrinsic loss and the output variation.

Subsystem Level Testing

After completion of the component level testing, the transmission interconnect hardware will be fully characterized.

Transmitter. With the calibrated amplifier, each transmitter will be measured to determine the amplitude and frequency characteristics of the electrical-to-optical-transfer function. Transmitter noise will also be measured.

Receiver. Receiver preamplifier characteristics will be measured in detail before component level tests are commenced. These measurements will include:

- Transimpedance/bandwidth characteristics
- RMS noise/bandwidth characteristics

Total receiver characteristics will then be measured at the point where the amplified pulses are fed into the comparator. These measurements will include:

- Amplification/bandwidth characteristics
- Noise/bandwidth characteristics
- Dynamic range

From the amplification and noise measurements, receiver sensitivity will be calculated.

Link Measurements. With a representative transmitter and receiver pair interconnected with the optical transmission system, total delay through the transmission interconnect will be measured for path configurations composed of representative lengths of cable. At the output of the PPM-to-Manchester conversion circuitry, pulse distortion and jitter as functions of optical signal level will be measured.

Laboratory-System-Level Testing Requirements

Once component and subsystem level testing is complete, laboratory-system-level testing will begin. This testing will be done in two parts: The wire system will be tested to establish a baseline and the fiber-optic system will be installed and tested. A comparison will then be done to measure the change in performance caused by the fiber-optic system. The test of each system will consist of running the A7 avionics program.

Bit Error Rate. Once functional operation of the fiber-optic (FO) bus has been demonstrated in the system, the bit error rate (BER) of the receiver will be determined in the laboratory setup shown in figure 9. In this arrangement, a constantly changing pattern, repeating every 16 bits or 16 μ s, is encoded into Manchester format and used as the input to the FO module. The output of the FO module (received data) is sent back to the logic where it is logically compared to the data sent out. To be considered valid, the received data must be true Manchester, i.e., bipolar and comparable with the data output to the FO module.

Both the total number of bits and the number of errors are brought out and accumulated in laboratory counters.

Once the setup is operating properly, the receiver threshold will be externally lowered until errors start to occur. The error count, bit count, and SNR will then be recorded and used to verify the calculated BER. Extrapolation to BER 10^{-12} will be made.

Intermessage Dynamic Range. The sensitivity of the receiver design to fast changes in average received signal level will be measured. This can be accomplished by keying two transmitters with drastically different optical path losses to one receiver. In this case, synchronization recognition, pulse distortion, and jitter will be the parameters of interest.

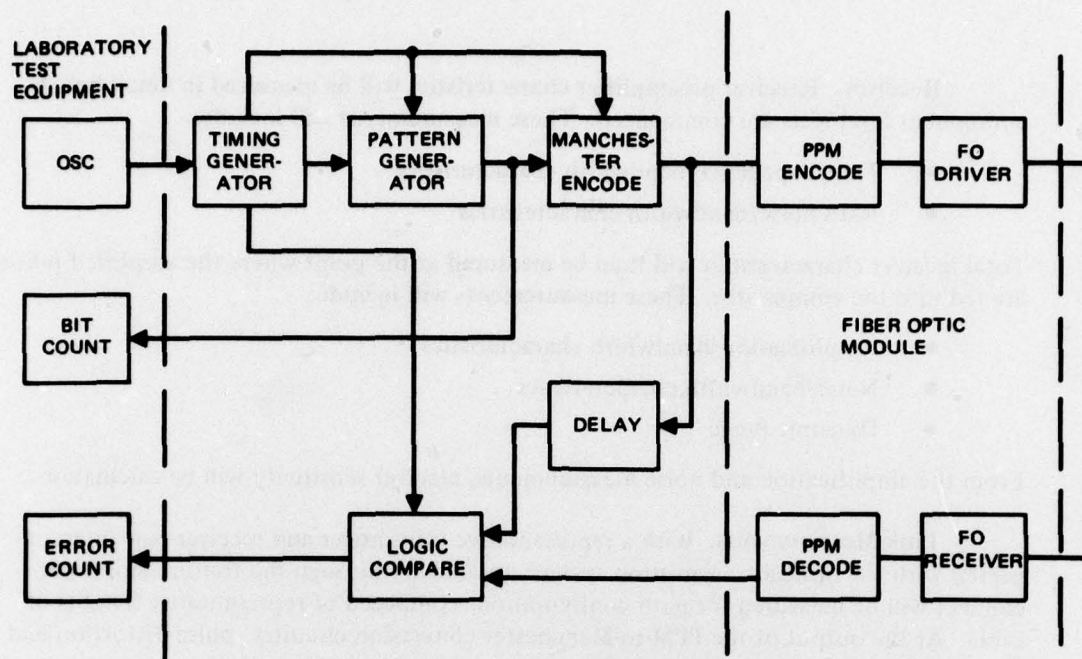


Figure 9. Bit error rate test setup.

Changes in these parameters will be measured when transmission is switched, within the minimum intermessage gap time specified in 1553, between transmitters.

Gap Times. The gap times specified in 1553 – intermessage gap time, terminal response time, and maximum no-response time out – will be measured between the points in a transmitter and receiver where the unipolar electrical Manchester signals exist, e.g., between the input to the encoder and the output of the decoder.

A7 Avionics Test Program. The A7 avionics test program will be used to measure the bus performance in a simulated system environment. This program will make extensive use of the SDL to simulate avionics units in the A7 aircraft.

A7 Avionics Test Inputs. These inputs will come from two sources: the SDL simulation and the A7 navigation weapon panel. Table 10 lists the units and parameters that the SDL simulates, and the parameters generated by the A7 navigation weapon panel are as follows:

- Present position latitude
- Present position longitude
- Update modes
- Destination coordinates
- Gyro bias drifts
- Accelerometer bias corrections
- Wind information

- LORAN or TACAN station insert data
- Mark data for coordinates of overfly position

Table 10. Simulated inputs parameters from SDL.

Unit	Parameter
Radar altimeter	Altitude
Doppler radar	Status
	Ground speed
	Drift angle
Forward-looking radar	Slant range to target
Air data computer	True airspeed
	Mach number
	Pressure altitude
Angle-of-attack sensor	Controls
	Angle of attack
Inertial measurement system	Pitch
	Roll
	True heading
	Magnetic heading
	Discretes
	Accelerometer X
	Accelerometer Y
	Accelerometer Z
	Gyro X
	Gyro Y
	Gyro Z

A7 Avionics Test Timing. Table 11 lists the bus transfers that take place and their rates. With these transfer rates the bus is loaded to 6.7 percent of its capacity.

A7 Avionics Test Outputs. These outputs will be in four units: the SDL (table 12), navigation weapon panel, head-up display, and ML1 computer. System performance parameters will also be calculated in the SDL. During the test, the SDL will calculate aircraft positional accuracy and weapon release point accuracy scoring.

Outputs to the navigation weapon panel are range to selected destinations, bearing to selected destination, and wind information. Outputs to the head-up display include attitude, heading, steering error, and altitude. The bus parameters that the ML1 computer monitors are as follows: bus parity, bus Manchester encoding, word count, synchronized waveform, word length, bus time out, and status word.

Table 11. Bus transfers.

Type*	Rate Messages per Second	Number of Words per Message	Data Source	Data Sink
RT-RT	20	8	SDL	TC2
RT-RT	20	8	SDL	TC2
RT-RT	20	15	SDL	TC2
RT-RT	20	6	TC2	SDL
RT-RT	20	11	TC2	SDL
RT-RT	20	8	TC2	SDL
RT-RT	5	4	SDL	TC2
RT-RT	10	32	TC2	SDL
RT-RT	10	32	TC2	SDL
RT-RT	3	32	TC2	SDL
RT-RT	3	32	TC2	SDL
RT-RT	3	32	TC2	SDL
RT-CT	1	32	SDL	ML1
CT-RT	As Required	32	ML1	SDL
RT-CT	10	16	SDL	ML1
CT-RT	10	16	ML1	SDL
RT-CT	10	16	TC2	ML1
CT-RT	5	16	ML1	TC2

*RT-RT Remote terminal to remote terminal transfer

RT-CT Remote terminal to controller transfer

CT-RT Controller to remote terminal transfer

Table 12. Simulated outputs parameters to SDL.

Unit	Parameter
Inertial measurement system	Discretes Gyro torquing X Gyro torquing Y Gyro torquing Z
Horizontal situation indicator/ attitude direction indicator	Range to destination Bearing to destination Ground track Steering error
Forward-looking radar indicator	Ground track velocity Flight path angle Drift angle Azimuth steering command Discretes Ground range to target True bearing
Flight recorder	

BREADBOARD DESIGN REPORT

This report details the electrical interface requirements for the transmitter and receiver designs to be used in the system demonstration.

The electrical design is based upon suitable interfaces available within the existing 1553 hardware in IBM's SIF laboratory. Both the transmitting and receiving interfaces are two-level Manchester logic waveforms. These waveforms are encoded to and decoded from a PPM Manchester.

Encoder Logic

The encoder logic converts from a TTL logic level Manchester waveform to a TTL logic level PPM waveform (see figure 10). The encoder receives the Manchester waveform, and the rising edge of the waveform enables a timer which samples the Manchester signal every 500 ns. If the sample output is a logic one, a 50-ns pulse is triggered from a single shot; if the sample output is a logic zero, the output does not change.

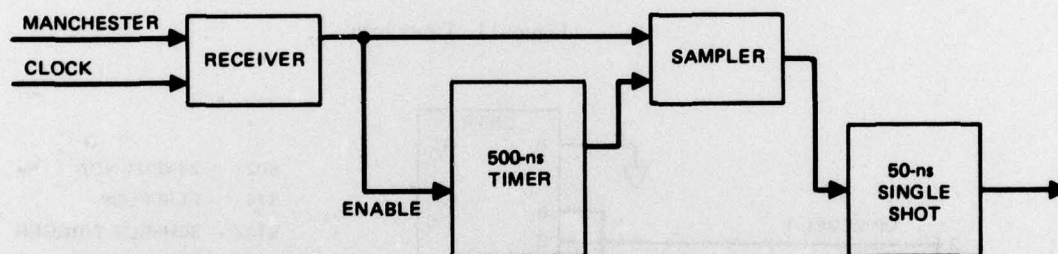


Figure 10. Encoder block diagram.

The timing for the 500-ns timer, the sampler, and the 50-ns single shot are derived from a 20-MHz (0.005 percent) crystal oscillator (figure 11). The detailed logic of the encoder is shown in figure 12.

Optical Driver Circuit

Figure 13 shows the driver's schematic with the selected component values. T1, T2, T3, T4, and T5 are an array of transistors on a single chip. D1, D2, D3, and D4 are diodes on a single chip array whose characteristics match those of the base emitter diode of the transistors. Transistor T1 is normally biased on to maintain the voltage on the base of T2 and T3 at a level that keeps the emitters of T2 and T3 near ground. This in turn keeps the gate voltage on the VMOS power FET at such a level that there is little if any conduction from source to drain. Transistor T5 is normally biased so that its collector voltage, which determines the emitter voltage of T4, will maintain a given charge on the 2- μ F capacitor C1. This charge is normally around +5 V. Approximately 0.5-mA will therefore flow through the 2231 LED to prebias it and will produce the minimum rise-time light output when turned on by the pulsed input. This is accomplished as follows: When the input pulse for the negative logic level turns transistor T1 off, the voltage on the base of T2, T3 rises and causes its emitter(s) to turn on the power FET. The FET's impedance from drain to source

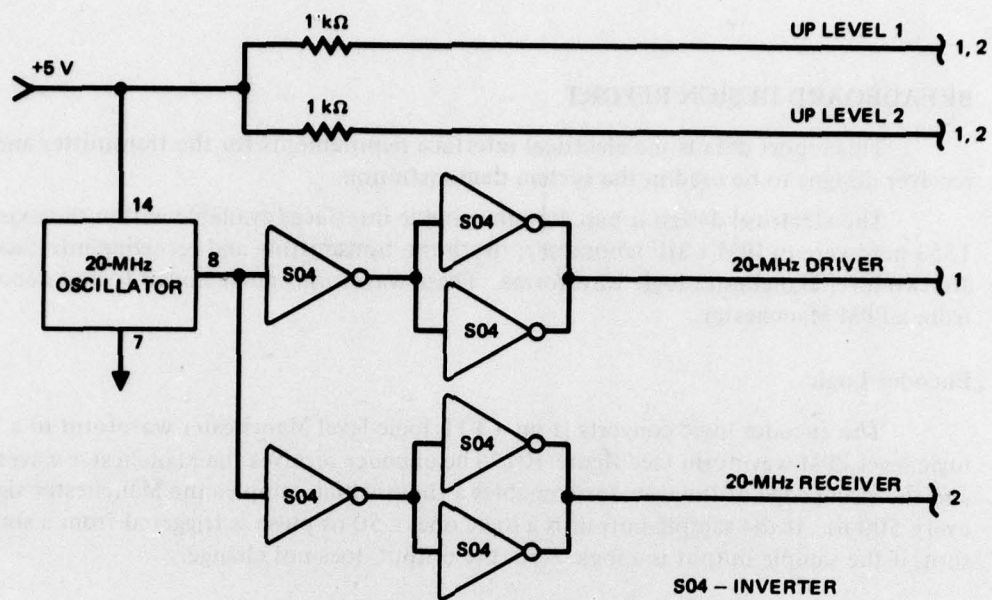


Figure 11. Timer logic.

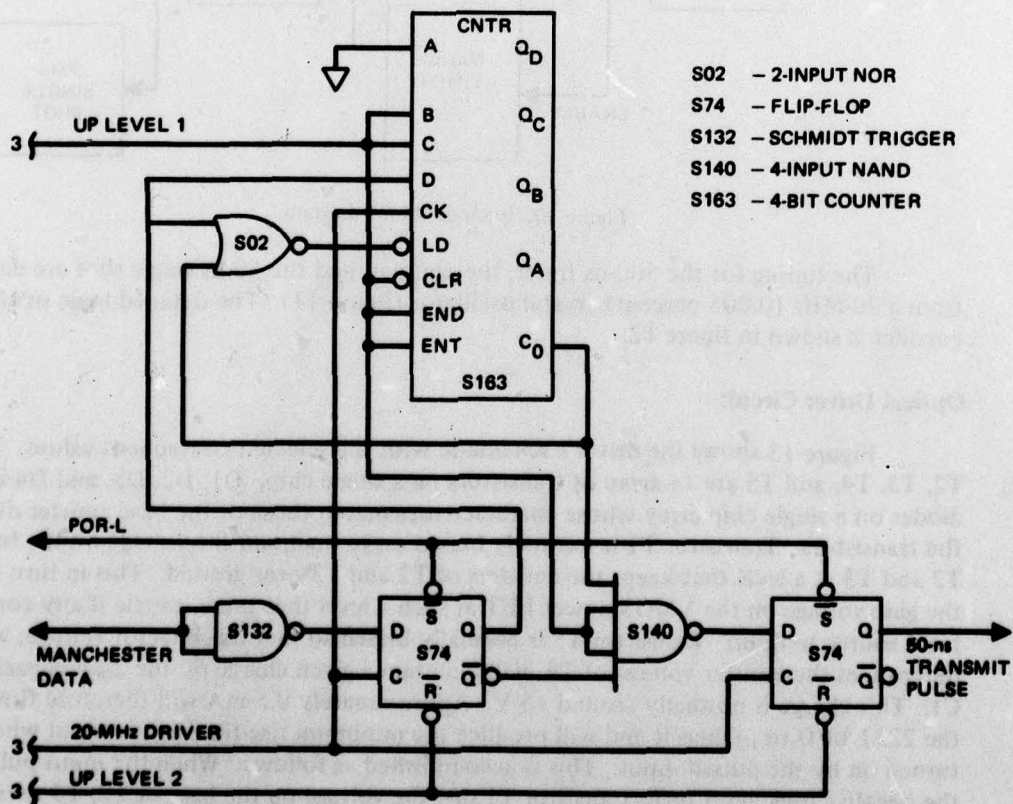


Figure 12. Encoder logic.

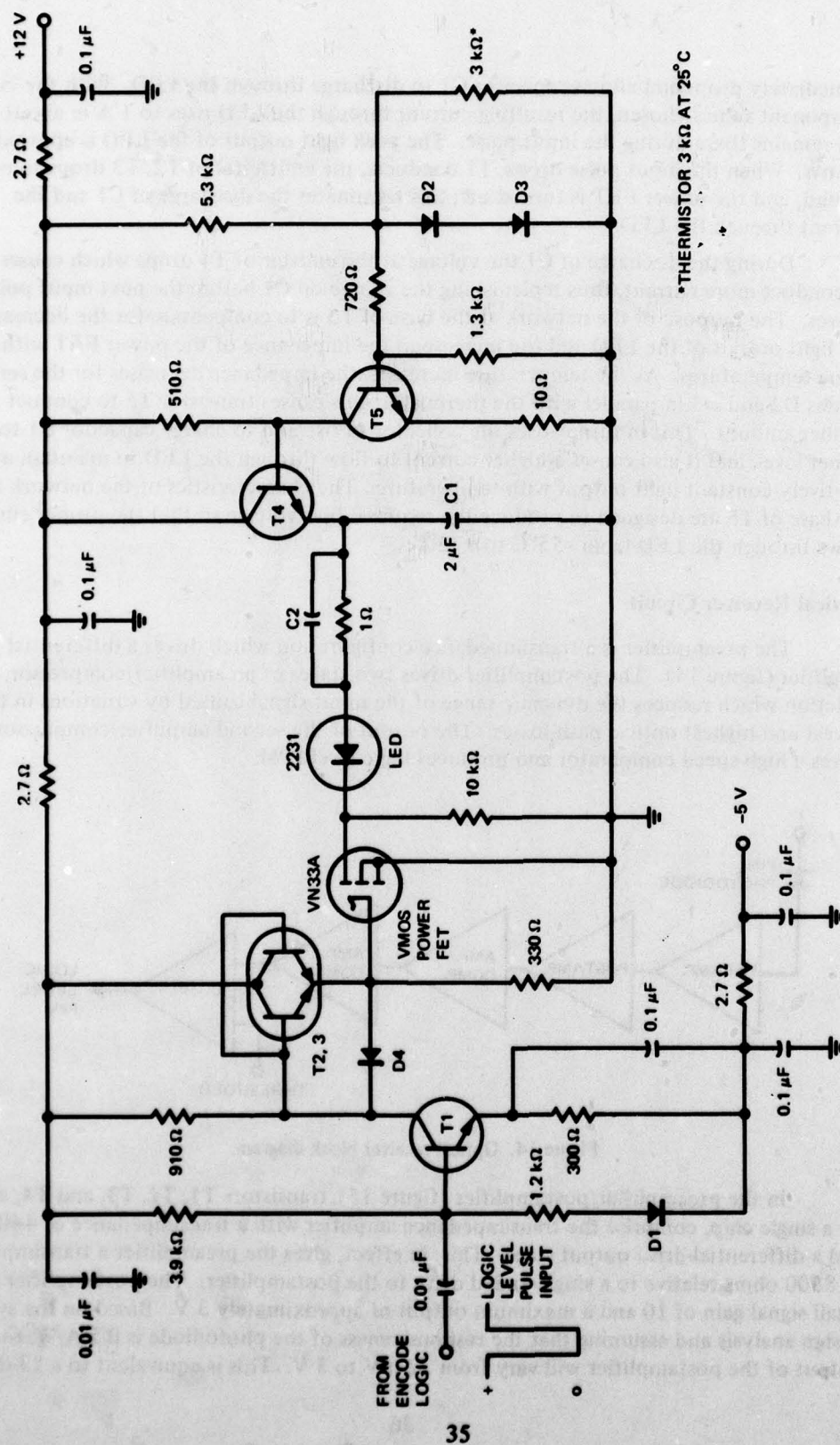


Figure 13. Optical driver circuit.

immediately drops and allows capacitor C1 to discharge through the LED. With the circuit component values chosen, the resulting current through the LED rises to 1 A in about 10 ns and remains there during the input pulse. The peak light output of the LED is approximately 10 mW. When the input pulse drops, T1 conducts, the emitter(s) of T2, T3 drops to near ground, and the power FET is turned off; this terminates the discharge of C1 and the current through the LED.

During the discharge of C1 the voltage at the emitter of T4 drops which causes it to conduct more current, thus replenishing the charge on C1 before the next input pulse arrives. The purpose of the network at the base of T5 is to compensate for the decrease in the light output of the LED and the increase in the impedance of the power FET with rising temperatures. As the temperature increases, the impedance decreases for the series diodes D2 and D3 in parallel with the thermistor; this causes transistor T5 to conduct a smaller amount. This in turn causes the collector to rise and to charge capacitor C1 to a higher level, and it also causes a higher current to flow through the LED to maintain a relatively constant light output with temperature. The characteristics of the network at the base of T5 are designed to produce the required bias voltage so that the proper current flows through the LED from -55°C to $+72^{\circ}\text{C}$.

Optical Receiver Circuit

The preamplifier is a transimpedance configuration which drives a differential post-amplifier (figure 14). The postamplifier drives two stages of an amplifier/compressor, a function which reduces the dynamic range of the input signal caused by variations in the lowest and highest optical path losses. The output of the second amplifier/compressor drives a high-speed comparator and produces logic level PPM.

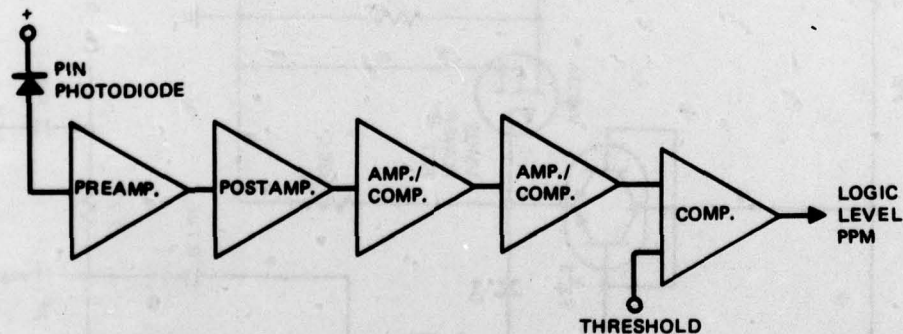
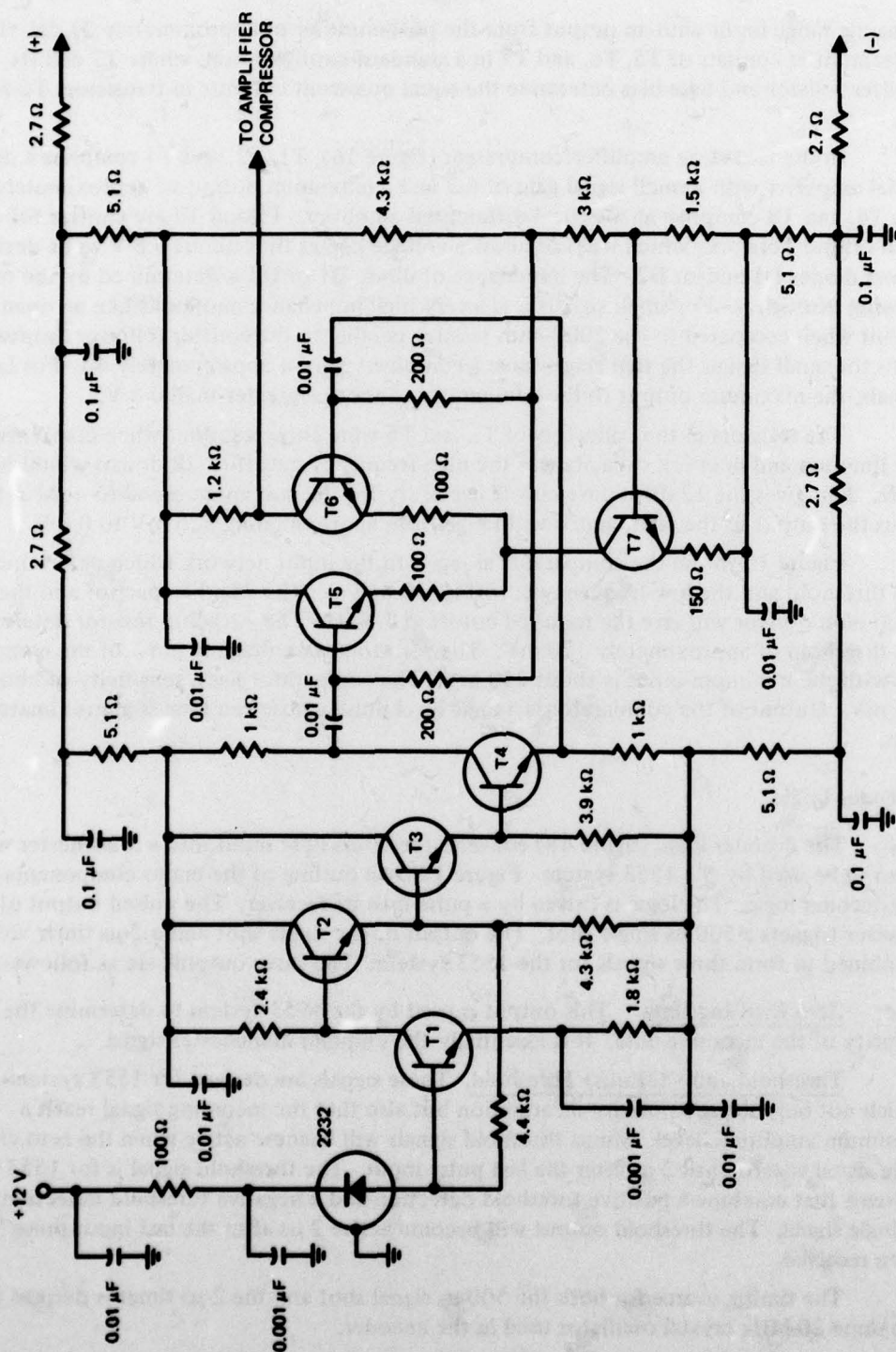


Figure 14. Optical receiver block diagram.

In the preamplifier/postamplifier (figure 15), transistors T1, T2, T3, and T4, an array on a single chip, comprise the transimpedance amplifier with a transimpedance of 4400 ohms and a differential-drive output stage. This, in effect, gives the preamplifier a transimpedance of 8800 ohms relative to a single-ended drive to the postamplifier. The postamplifier has a small signal gain of 10 and a maximum output of approximately 3 V. Based on the system design analysis and assuming that the responsiveness of the photodiode is 0.5 A/W, the output of the postamplifier will vary from 22 mV to 3 V. This is equivalent to a 23-dB



dynamic range input with an output from the postamplifier of approximately 21 dB. The postamplifier consists of T5, T6, and T7 in a standard configuration, where T7 and its emitter resistor and base bias determine the equal quiescent currents in transistors T5 and T6.

In the two-stage amplifier/compressor (figure 16), T1, T2, and T4 comprise a differential amplifier with a small signal gain of 6.3 and a maximum output of approximately 4 V. T5, T6, and T8 comprise an identical differential amplifier. T3 and T7 are emitter followers with output networks which will not allow a voltage higher than about 0.8 V to be developed across diodes D1 and/or D2. The impedance of diode D1 or D2 is determined by the current flowing through it. For small signals it is a very high impedance and looks like an open circuit when compared to the 2000-ohm resistor parallel to the emitter follower output. Thus for small signals the two stages have a combined gain of approximately 40. For larger signals, the maximum output to the comparator cannot be greater than 0.8 V.

The resistors in the collectors of T2 and T6 were chosen so that when combined with the junction and network capacitances the high-frequency cutoff (3 dB down) would be 8 MHz. This gives the 12-dB/octave cutoff necessary for the maximum signal-to-noise ratio. Thus the output to the comparator will range from approximately 325 mV to 0.8 V.

Figure 17 shows the comparator along with the input network which determines the threshold and the low-frequency cutoff (3 dB down). The 75-pF capacitor and the 2000-ohm resistor will give the required cutoff at 1 MHz. The 120-ohm resistor determines the threshold of approximately 120 mV. The zero-to-peak voltage at pin 1 of the comparator with the minimum input is about 240 mV. The comparator has a sensitivity of about 0.5 mV. Output of the comparator is a logic level pulse whose rise time is approximately 2 ns.

Decoder Logic

The decoder logic (figure 18) converts the 50-ns PPM input into a Manchester waveform to be used by the 1553 system. Figure 19 is an outline of the major components of the decoder logic. The logic is driven by a pulse into its receiver. The pulsed output of the receiver triggers a 500-ns single shot. The output of the single shot and a 2- μ s timer are combined to form three signals for the 1553 system. The three outputs are as follows:

Zero Crossing Data This output is used by the 1553 system to determine the polarity of the incoming data. It is essentially the unipolar Manchester signal.

Threshold and - (Minus) Threshold. These signals are derived for 1553 systems which not only require polarity information but also that the incoming signal reach a minimum amplitude level. Minus threshold signals will become active when the zero crossing data signal is zero until 2 μ s after the last pulse input. The threshold signal is for 1553 systems that combine a positive threshold detection and a negative threshold detection into a single signal. The threshold output will become active 2 μ s after the last input pulse has been received.

The timing source for both the 500-ns signal shot and the 2- μ s timer is derived from the same 20-MHz crystal oscillator used in the encoder.

The outputs of the decoder will be TTL voltage compatible and source 20 mA into the load and sink 20 mA from the load.

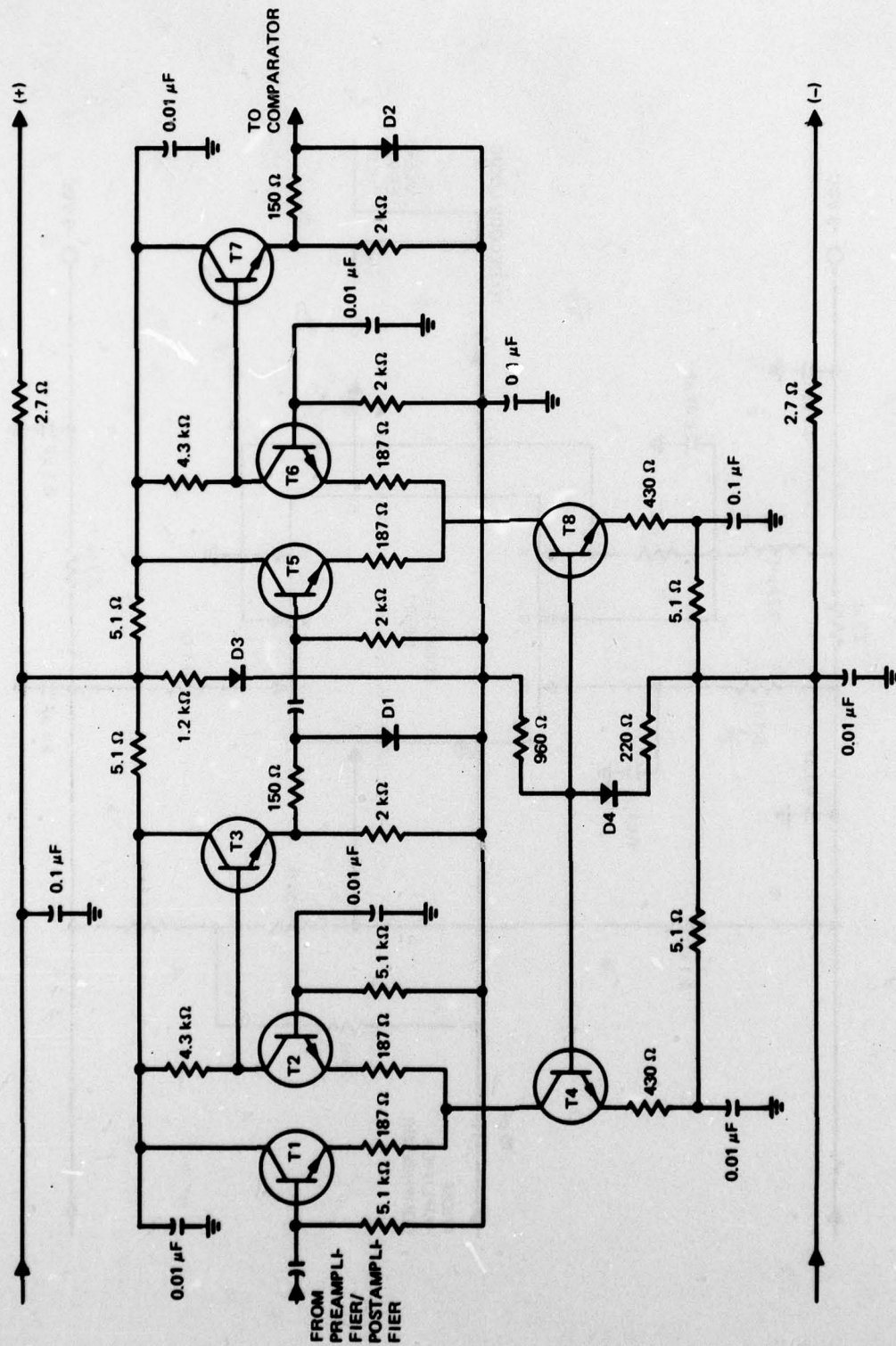


Figure 16. Amplifier compressor.

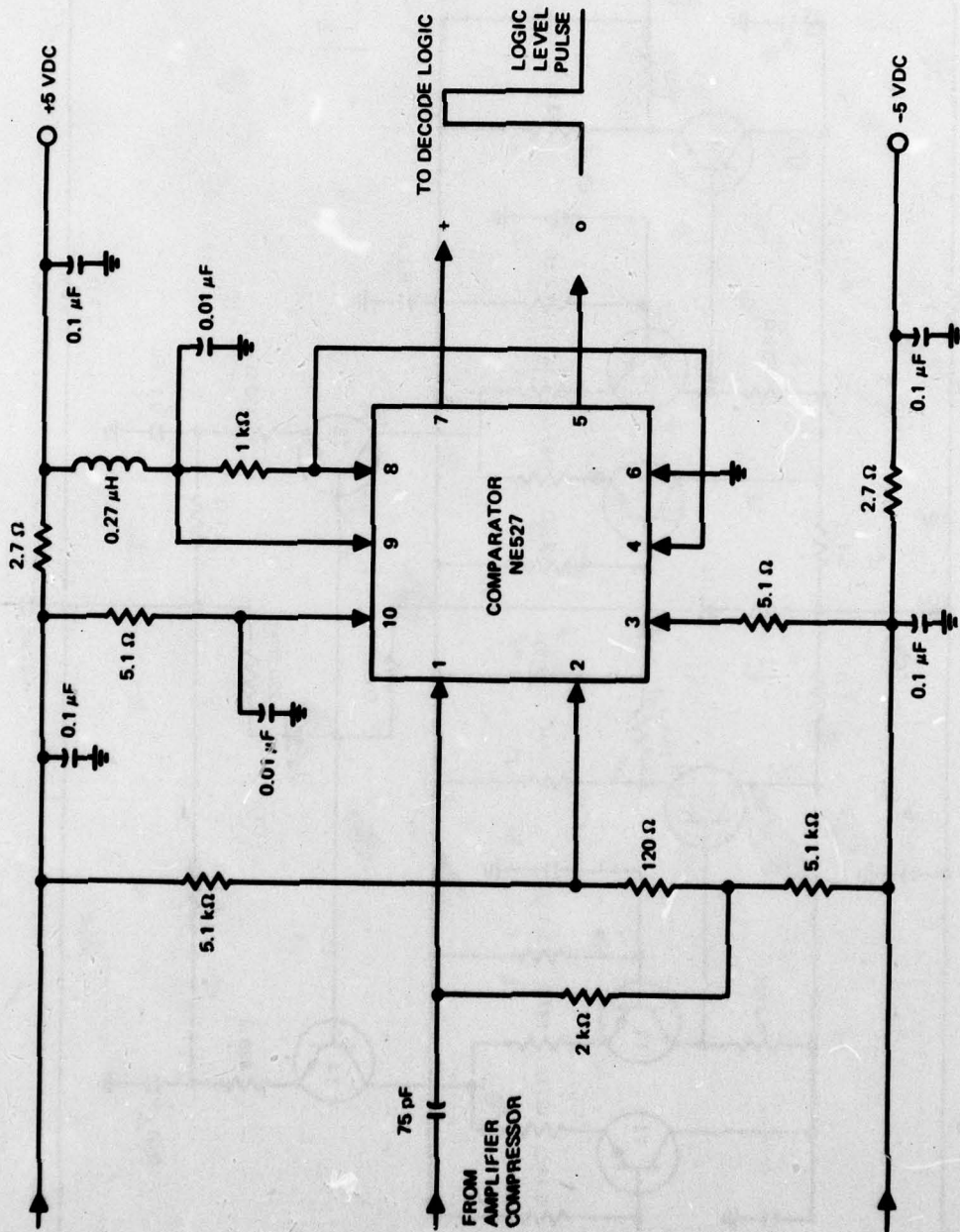


Figure 17. Threshold network and comparator.

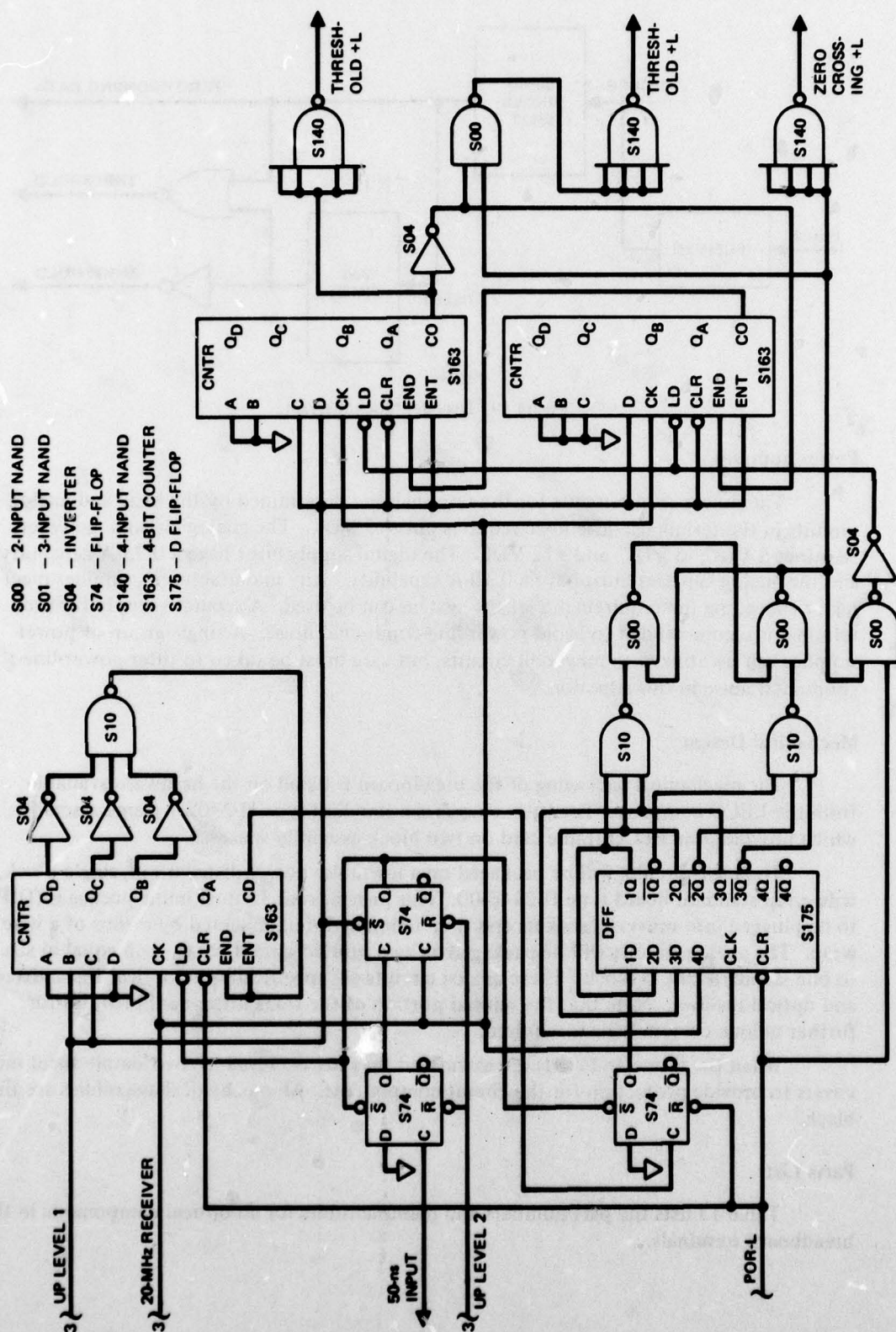


Figure 18. Decoder logic.

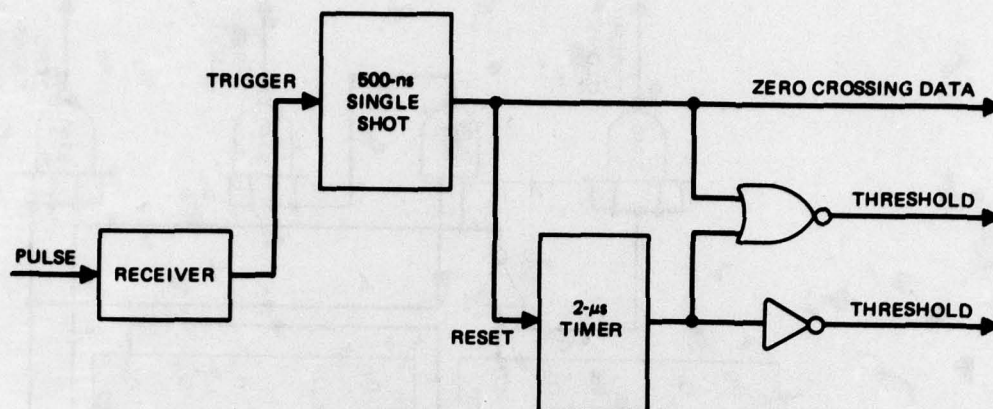


Figure 19. Decoder block diagram.

Power Supplies

The power requirements for the terminals are determined by the logic and analog circuits in the terminals. The logic requires only +5 VDC. The analog circuits, however, require +5 VDC, -5 VDC, and +12 VDC. The digital supply must have a 0.75-A capability and the analog supplies must have a 0.10-A capability. Any manufacturer's supplies meeting or exceeding the requirements of the system can be used. A separate supply for each terminal is recommended to avoid power-line-conducted noise. A single group of power supplies can be utilized to power all circuits, but care must be taken to filter power-line-conducted noise in this situation.

Mechanical Design

The mechanical packaging of the breadboard is based on the hardware available from the EECO company. The basic chassis is a standard type H-2308-1 frame assembly, which provides one EECO frame card on two block assembly spaces.

The logic circuits will be packaged on a low-noise power distribution, single-block, wire-wrap standard board type H-2948-00. This provides for 18 dual inline packages (DIPs) to be plugged into universal sockets and then uniquely interconnected by means of a wire wrap. The analog circuits will be packaged on two printed circuit cards, each equal in size to one standard EECO block. These analog circuits are specifically the optical transmitter and optical receiver. Note that the unused portion of the transmitter card provides for further unique custom logic if required.

When the frame and cards are assembled they are enclosed by two simple sheet metal covers to provide protection for the circuit components. All mechanical assemblies are flat black.

Parts List

Table 13 lists the part numbers and manufacturers for all optical components in the breadboard terminals.

Table 13. Optical components: parts list.

Description	Manufacturer, Part Number	Number Required
Light-emitting diodes	Spectronics, SE2231-003	3
Photodiodes	Spectronics, SD3478-002	3
Coupler	Spectronics, SPX-3028-161	1
Fiber-optic cable (per quote R-5341A, item 1; 300 m)	ITT, ESM-10-PS	1
Cable connectors (hexagonal, key modified)	ITT, MIL-C-85044	18
Feed-through con- nectors (hexagonal, key modified)	ITT, MIL-C-85044	6
Device connectors (hexagonal, key modified)	ITT, MIL-C-85044	6

Electrical parts are as follows:

Encoder Logic, Decoder Logic, Timer

1	74S00	} integrated circuits
1	74S02	
2	74S04	
1	74S10	
3	74S74	
1	74S132	
2	74S140	
4	74S163	}
1	74S175	
1	20-MHz oscillator	
2	1000-ohm 0.25-W resistors	

Analog Driver

1	3045 transistor array
1	3019 diode array
1	VN33A VMOS power FET

- 1 SP2231 LED (also shown in optical parts)
- 15 0.25-W film resistors
- 8 Ceramic capacitors
- 1 3000-ohm thermistor

Analog Receiver

- 1 3018 transistor array
- 3 3045 transistor arrays
- 1 3019 diode array
- 1 SD3478 photodiode (also shown in optical parts)
- 1 NE527 comparator
- 1 0.27- μ F inductor
- 56 0.25-W film resistors
- 29 Ceramic capacitors

Power Supplies

- 1 +12-, +5-, -5-VDC supply at 0.1, 0.75, 0.1 A, respectively

Mechanical parts are listed in table 14.

Table 14. Mechanical components: parts list.

Description	Manufacturer, Part Number	Number Required
Frame assembly	EECO, H-2308-01	1
Socket board	EECO, H-2948-00	1
Analog printed circuit card	IBM	1
Cover - component side (frame)	IBM, H-2308-01	1
Cover - wire side	IBM, H-2308-01	1

REFERENCES

1. Naval Ocean Systems Center, Technical Document 197, Avioptics Program Plan, W. J. Tinston, Jr., 25 September 1978.
2. Naval Electronics Laboratory Center, Technical Report 1982, A-7 ALOFT Life-Cycle Costs and Measures of Effectiveness Models, R. A. Greenwell, March 1976.
3. IBM, Report 77-560-001, System Documentation Report of Software Integration Facility: Summary Report, P. A. Wilkinson, 14 October 1977.
4. IBM, Report 78-A59-003, Fiber Optic Interconnect Systems: System Analysis Report, R. Betts and R. C. Clapper, 16 March 1978.

5. IBM, Report 78-A77-001A, Development and Test Plan for MIL-STD-1553 Compatible Fiber Optic System, V. P. Zeyak, Jr., and R. Betts, 22 March 1978.
6. IBM, Report 78-517-002, Breadboard Design Report, R. Betts, 6 November 1978.
7. Standard Telecommunications Laboratory, The Phenomenon of Modal Noise in Analogue and Digital Optical Fiber Systems, R. E. Edworth, 1978.
8. Proceedings of the IEEE, vol. 61, no. 12, pp. 1727-1730, "Research Toward Optical-Fiber Transmission Systems, Part II," S. Miller, T. Li, and E. A. J. Marcatili, December 1973.
9. RCA, Reprint RE-20-2-13, Optical Fiber Communications Systems, J. D. Wittke, February 1974, pp. 25-27.
10. AFAL, AFAL-TR-75-45, Optoelectronic Aspects of Avionic Systems, Vol. II, J. R. Biard, May 1975, pp. 70-78.
11. Applied Optics, vol. 15, no. 1, p. 252, "Optical Access Couplers and a Comparison of Multiterminal Fiber Communication Systems," A. F. Milton and A. B. Lee, January 1976.
12. IBM, Report 75-70-00436, Analysis and Selection of the Physical Parameters of an Optical-Fiber Bundle, R. C. Clapper and R. Betts, October 1975.
13. Draft MIL-STD-1553B, Aircraft Internal Time Division Command/Response Multiplex Data Bus, 16 June 1978, Sections 4-3-4.4.
14. Spectronics, Inc, Thermal Transients in Light Emitting Diodes, J. R. Biard, 1978. Figure 10.